

Review

Open Access



# Recent progress of decacarbonyldimanganese catalysis

Tao Li<sup>1</sup>, Albert S. C. Chan<sup>1,2,3</sup>, Shan-Shui Meng<sup>3,\*</sup>

<sup>1</sup>Chongqing Institute of Green and Intelligent Technology, Chongqing School, University of Chinese Academy of Sciences (UCAS Chongqing), Chongqing 400714, China.

<sup>2</sup>University of Chinese Academy of Sciences, Beijing 100049, China.

<sup>3</sup>School of Pharmaceutical Sciences, Sun Yat-sen University, Guangzhou 510006, China.

**Correspondence to:** Prof. Shan-Shui Meng, School of Pharmaceutical Sciences, Sun Yat-sen University, Waihuan Road, Guangzhou, 510006, China. E-mail: mengshsh@mail.sysu.edu.cn

**How to cite this article:** Li T, Chan ASC, Meng SS. Recent progress of decacarbonyldimanganese catalysis. *Chem Synth* 2023;4:43. <https://dx.doi.org/10.20517/cs.2023.32>

**Received:** 29 Jun 2023 **First Decision:** 17 Aug 2023 **Revised:** 15 Sep 2023 **Accepted:** 28 Sep 2023 **Published:** 11 Oct 2023

**Academic Editor:** Da-Gang Yu **Copy Editor:** Yanbing Bai **Production Editor:** Yanbing Bai

## Abstract

Decacarbonyldimanganese ( $Mn_2(CO)_{10}$ ), one of the most long-standing organometallic reagents, bears a weak Mn-Mn bond, which occurs a homo-cleavage feasibly under heating or light-irritation, delivering an active manganese-centered radical. This highly reactive metallic radical could activate the Si-H bond, C-halogen bond, N-halogen bond, S-halogen bond, and O=O bond, generating corresponding Mn species and Si, C, N, S, and O radicals. This wonderful reactivity enables an extensive utilization of this dimeric manganese in catalytic atom-transfer reactions and oxidation reactions. In this review, we offer a comprehensive review of this growing area in recent decades. Critical comparisons and mechanism analyses are provided, along with personal perspectives for future studies.

**Keywords:** Decacarbonyldimanganese, atom-transfer reaction, light-irritation, dinuclear-metal catalysis, single-electron oxidation

## INTRODUCTION

Manganese, one of the most representative 3d metals, possesses the third most abundance in the earth-crust<sup>[1]</sup>. It possesses a range of appealing chemical properties, including environmental and biological compatibility, high potential for redox activity with multiple oxidation states (-3 to 7), and the ability to break the trend of electronegativity due to the half-shell effect<sup>[2,3]</sup>. Consequently, manganese catalysis has



© The Author(s) 2023. **Open Access** This article is licensed under a Creative Commons Attribution 4.0 International License (<https://creativecommons.org/licenses/by/4.0/>), which permits unrestricted use, sharing, adaptation, distribution and reproduction in any medium or format, for any purpose, even commercially, as long as you give appropriate credit to the original author(s) and the source, provide a link to the Creative Commons license, and indicate if changes were made.



emerged as a promising alternative to noble-metal catalysis. Moreover, the abundance, low cost, and low toxicity of manganese make it an attractive option for various industrial applications. In recent years, there have been significant advancements in developing new catalytic reactions based on manganese complexes, including oxidative coupling reactions<sup>[4]</sup>, C-H functionalization reactions<sup>[5,6]</sup>, asymmetric catalysis, and other important organic transformations<sup>[7-9]</sup>. These advances have led to significant progress in the field of organic synthesis, which has the potential to revolutionize drug development and other applications. Ackermann<sup>[10]</sup>, Shenvi<sup>[11]</sup>, Trovitch<sup>[12]</sup>, Wang<sup>[6]</sup>, and Srimani<sup>[13]</sup> have recently published excellent reviews focusing on the development of Mn-catalysis, providing comprehensive insights into this rapidly evolving field.

Decacarbonyldimanganese ( $\text{Mn}_2(\text{CO})_{10}$ ), comprised of two identical  $\text{Mn}^0$  atoms, is a long-standing organometal reagent. This dimeric manganese reagent features a central manganese atom that links one axial carbonyl and four equatorial carbonyls (the axial carbonyl exhibits greater thermal motion due to less steric hindrance), while the two metal centers are connected by a weak Mn-Mn homolytic bond [Bond dissociation energy (BDE) = 94-154  $\text{KJ}\cdot\text{mol}^{-1}$ ]<sup>[14,15]</sup>. Under specific temperature or light irradiation conditions, the homogeneous cleavage of the Mn-Mn single bond provides a highly reactive metal-centered radical species ( $\cdot\text{Mn}(\text{CO})_5$ ) [Figure 1]<sup>[16,17]</sup>. This 17-electron species readily abstracts hydrogen or halogen atoms from silanes or halogenoalkanes, generating  $\text{H-Mn}(\text{CO})_5$  or  $\text{X-Mn}(\text{CO})_5$  and corresponding silyl or alkyl radical intermediates. Thanks to its fantastic reactivity, the application of  $\text{Mn}_2(\text{CO})_{10}$  in the so-called atom-transfer reactions (ATRs) has obtained considerable advances in recent decades<sup>[18-25]</sup>. More recently,  $\text{Mn}_2(\text{CO})_{10}$ -mediated ATRs have also been explored for C-N construction, further enriching the arsenal of the introduction of N atoms to organic molecules<sup>[26-28]</sup>. The active metal radical could also capture molecular oxygen feasibly and produce a reactive superoxide radical species  $\text{Mn}(\text{CO})_5\text{OO}\cdot$ , which has been observed and characterized by Mach *et al.*<sup>[29,30]</sup> clearly. In theory, this superoxide radical could be used as an effective oxidant to realize single-electron oxidation of organic molecules. However, only limited studies have been conducted on the application of the superoxide radical since its discovery by Mach<sup>[31,32]</sup>.

With this review, we present a comprehensive overview of the progress in the area of  $\text{Mn}_2(\text{CO})_{10}$ -catalyzed ATRs and oxidation reactions over the past decade. This review is divided based on the type of chemical bonds activated by  $\text{Mn}_2(\text{CO})_{10}$ , and detailed mechanisms of these reactions are also described and discussed. We aim to provide readers with a profound understanding of the catalytic model of the dinuclear manganese reagent and, consequently, stimulate further and deeper development in this important area.

## MAIN TEXT

### Activation of Si-H bond

Metal-catalyzed hydrosilylation of alkynes is one of the most straightforward approaches to silyl-substituted alkenes with 100% atom economy. However, controlling the stereo- and regio-selectivity for unsymmetrical alkynes and avoiding the generation of hydrogenation byproducts remain two main challenges in the reaction. To address these challenges, Yang *et al.* developed a stereo-divergent hydrosilylation approach of alkynes through a mono- or di-manganese catalytic system in 2017 [Scheme 1]<sup>[33]</sup>. Initially, they found that  $\text{MnBr}(\text{CO})_5$  exhibited low conversion (25% yield) and E/Z selectivity (1.3:1) in the hydrosilylation reaction. To enhance both hydrosilylation efficiency and E-selectivity, they introduced triphenylarsine as the mononuclear manganese ligand. This modification significantly improved the E-selective hydrosilylation (3-1 to 3-9, up to 89% yield, up to > 50:1 E/Z). The regioselectivity, on the other hand, seemed only to correspond with the steric properties of the alkyne (3-8, 3-9). Interestingly, a reversed Z-selectivity was observed when the mono-manganese catalyst was replaced by  $\text{Mn}_2(\text{CO})_{10}$ . The Z-selectivity was obviously enhanced by the addition of dilauroyl peroxide (LPO), probably because the added peroxide accelerated the cleavage of the Mn-Mn bond. In the screening of silane scope, the use of more sterically bulky silanes

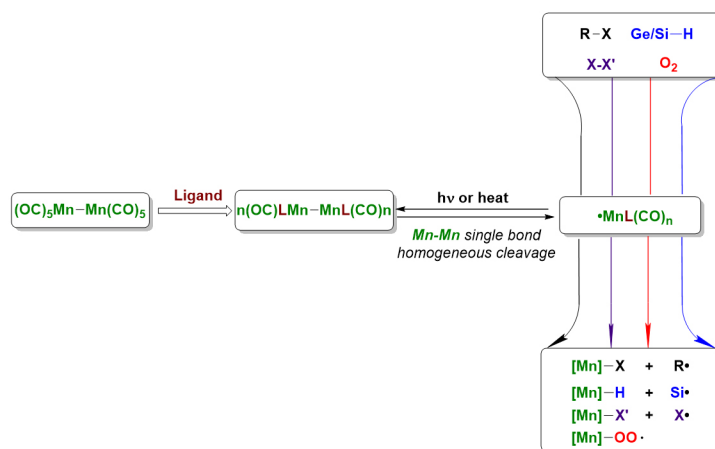
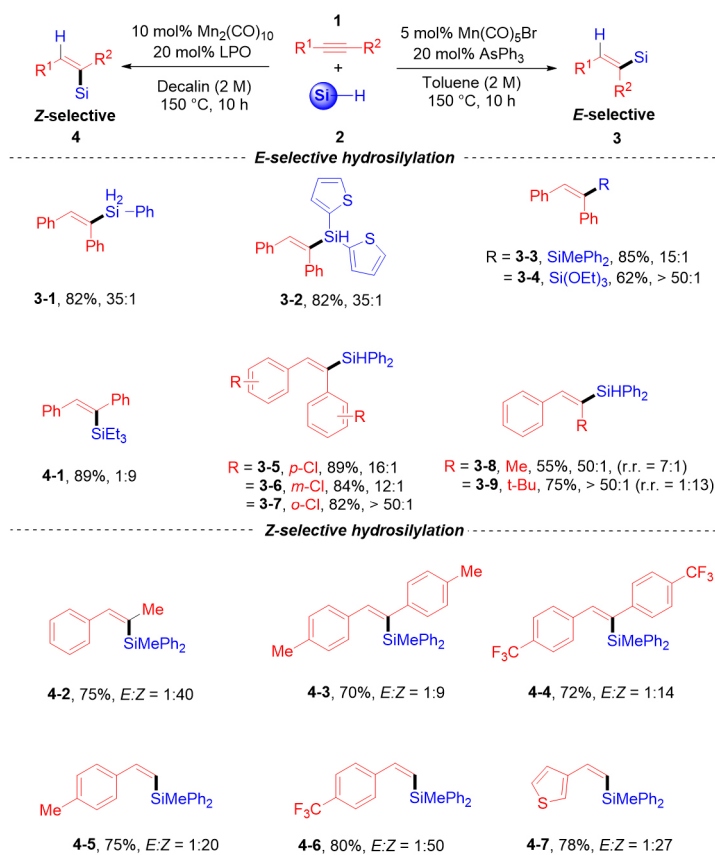


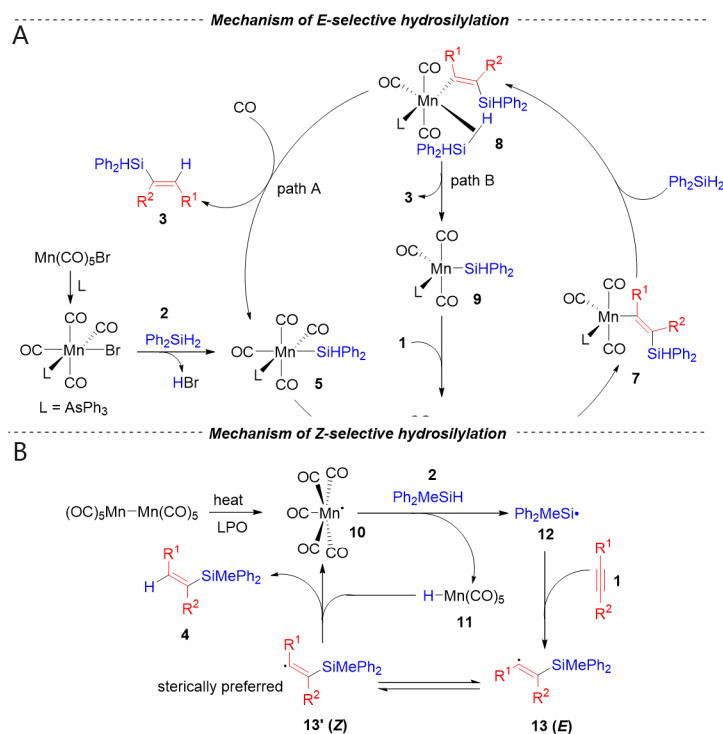
Figure 1. Diverse organic transformations mediated by  $\text{Mn}_2(\text{CO})_{10}$ .



Scheme 1. Direct hydrosilylation of alkynes by different manganese catalytic systems.

resulted in better *Z*-selectivity (4-2 to 4-7), while  $\text{Et}_3\text{SiH}$  consistently produced *Z*-product in both reaction conditions (4-1).

Based on controlled experiments, mechanisms of the two different stereoselective hydrosilylation reactions were proposed by the researchers [Scheme 2]. The real catalyst in the *E*-hydrosilylation was Mn-Si species 5,



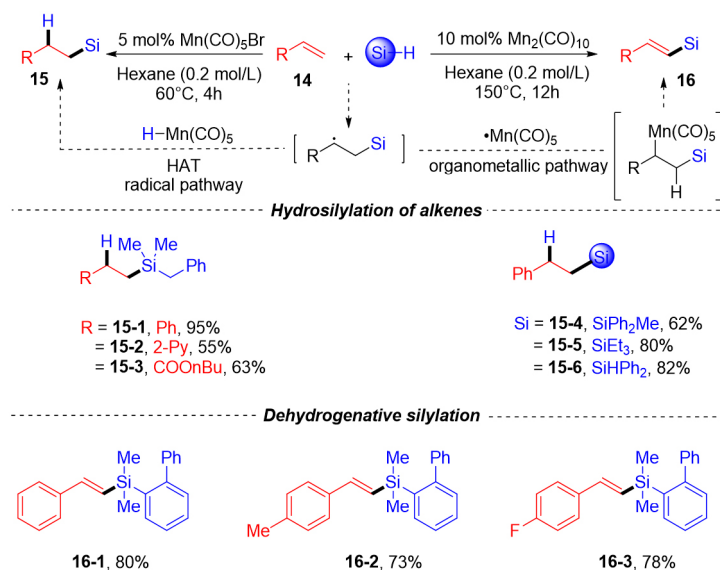
**Scheme 2.** The possible reaction mechanism of (A) *E*-configured product and (B) *Z*-configured product.

which was in-situ generated from  $\text{MnBr}(\text{CO})_5$  and silanes. Under heating conditions, an alkyne/ $\text{CO}$  exchange of 5 occurred, then the insertion of the alkyne moiety into the Mn-Si bond resulted in a ( $\beta$ -silyl) alkenyl-Mn intermediate 7. The coordination and  $\sigma$ -bond metathesis of 7 with silane led to product 3 and regenerated the Mn-Si catalyst, thus closing the catalytic cycle. Alternatively, species 8 might also release product 3 directly meanwhile delivering intermediate 9; after that, another alkyne molecule coordinated to 9, re-forming complex 6.

In *Z*-hydrosilylation, the initial Mn-Mn bond cleavage was facilitated by LPO, generating the reactive manganese radical 10. Subsequently, the Si-H bond was activated by 10, producing the free silyl radical 12 and Mn-H species 11, a following silyl radical addition to the alkyne, forming an unstable alkenyl radical 13. Due to the bulky steric hindrance of a diphenylmethylsilyl group, the H-atom transfer between the *Z*-configured alkenyl radical and  $\text{HMn}(\text{CO})_5$  was favored, leading to the final *Z*-alkenyl product.

Following the successful stereo-divergent hydrosilylation of alkynes, Yang *et al.* investigated the divergent silylation of alkenes [Scheme 3]<sup>[34]</sup>. Using  $\text{MnBr}(\text{CO})_5$  as the catalyst, the hydrosilylation and dehydrogenative silylation products of styrene were isolated at 38% yield and 7% yield at 150 °C, respectively. Lower reaction temperature (60 °C) or UV irradiation both promoted the hydrosilylation efficiently (15-1, 95% yield). Interestingly, the dehydrogenative silylation product became the main product under the catalysis of  $\text{Mn}_2(\text{CO})_{10}$  at a higher temperature (150 °C) with bulky silane. When excess alkene was added to the reaction and used as the hydrogen acceptor, the efficiency of dehydrogenative silylation was further enhanced. However, the substrate scope investigation revealed that the dehydrogenative silylation was strictly limited to bulky silanes and aryl olefins (16-1 to 16-3).



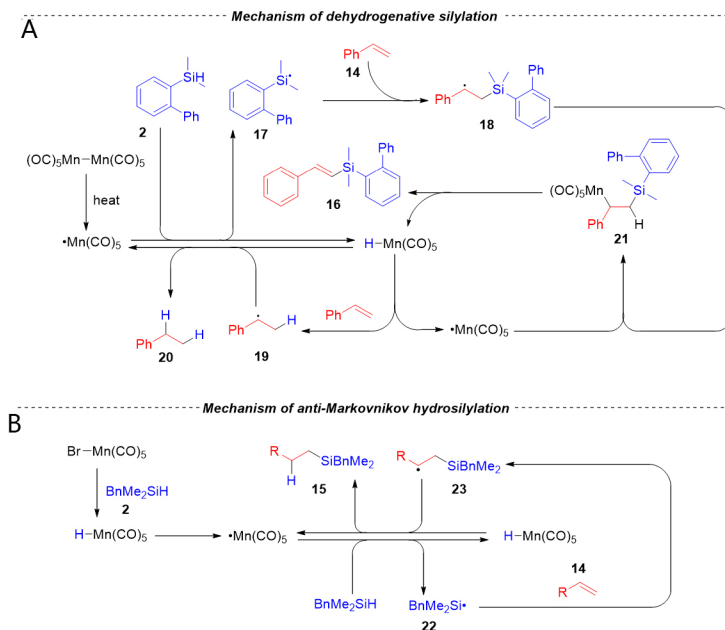


**Scheme 3.** Mn-catalyzed hydrosilylation and dehydrogenative silylation of alkenes.

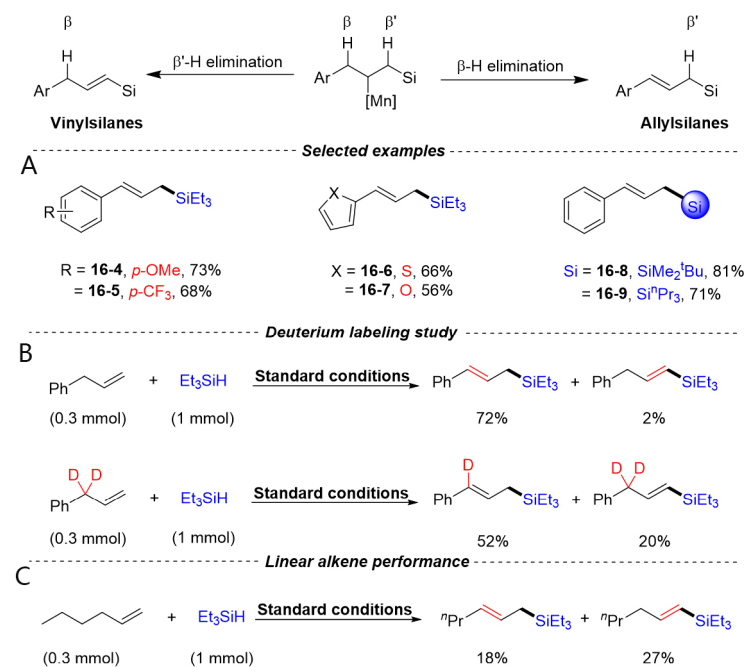
The authors conducted a series of mechanistic studies to clarify the divergent dehydrosilylation process. In [Scheme 4A](#), it was proposed that the  $\text{Mn}(\text{CO})_5$  radical abstracted H-atom of silane giving silyl radical 17 and  $\text{HMn}(\text{CO})_5$ , a  $\beta$ -silyl alkyl radical 18 was produced after the radical addition with an alkene substrate. The remaining  $\text{Mn}(\text{CO})_5$  radical coupled with 18, yielding the organomanganese intermediate 21. A subsequent  $\beta$ -H elimination led to the desired dehydrogenative product 16. In the anti-Markovnikov hydrosilylation process [[Scheme 4B](#)], the generated silyl radical 23 underwent a common hydrogen atom transfer (HAT) process with  $\text{HMn}(\text{CO})_5$ , resulting in the addition product 15.

Inspired by the  $\text{Mn}_2(\text{CO})_{10}$ -catalyzed dehydrogenative silylation, Wu *et al.* reasoned that the  $\beta$ -H elimination of the organomanganese intermediate would predominantly occur at the benzylic site, giving olefin migration products [[Scheme 5](#)]<sup>[35]</sup>. Unlike Wang's work,  $\text{Et}_3\text{SiH}$  and other less steric-hindered trialkylsilanes were workable in the synthesis of allylsilanes, a library of synthetic-valuable allylsilanes were smoothly produced (16-4 to 16-9, 56%-81% yield). When hexene was devoted to the reaction, a mixture of vinylsilane and allylsilane was obtained with low yields [[Scheme 5C](#)].

As in these precedents, the chemoselectivity was controlled by the steric-hindrance of silanes and different carbonylmanganese species, but dehydrosilylation selectivity was only up to 10:1. To address these limitations, Dong *et al.* reported an elegant ligand-controlled divergent silylation of alkenes only with dinuclear carbonylmanganese [[Scheme 6](#)]<sup>[36]</sup>. They disclosed that the dehydrosilylation of alkenes was well supported by the electron-rich bidentate  $\text{PrPNP}$  ligand (L1), while the relatively electron-deficient bidentate JackiePhos ligand (L2) selectively facilitated the hydrosilylation process [[Scheme 6](#)]. In the dehydrosilylation process, styrenes bearing different substituents (*ortho*-, *meta*-, and *para*-) (16-4 to 16-7) were all tolerated, as well as heteroaromatic (16-8, 16-9) and non-activated aliphatic alkenes (16-10, 16-11). It is worth noting that a competing  $\beta$ -H elimination occurred predominantly when aliphatic alkenes bear an acidic allylic  $\text{C}(\text{sp}^3)\text{-H}$  bond (16-12, 16-13). Tertiary silanes (16-14, 16-15) were tolerated well in the manganese-catalyzed dehydrosilylation, while primary and secondary silanes failed to generate the key silyl radicals under the optimal conditions (16-16, 16-17). In the hydrosilylation part, both aromatic and aliphatic alkenes were readily reacted with tertiary silanes in high efficiencies and excellent linear selectivity (linear: branch



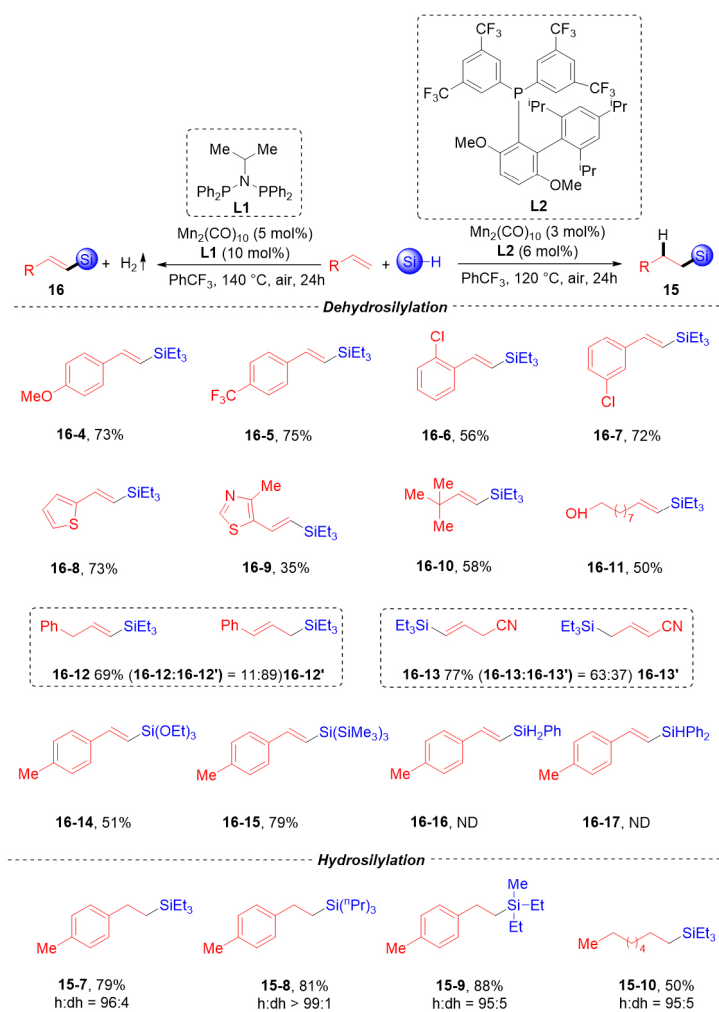
**Scheme 4.** (A) The possible reaction mechanism of dehydrogenative silylation; (B) Mechanism of anti-Markovnikov hydrosilylation.



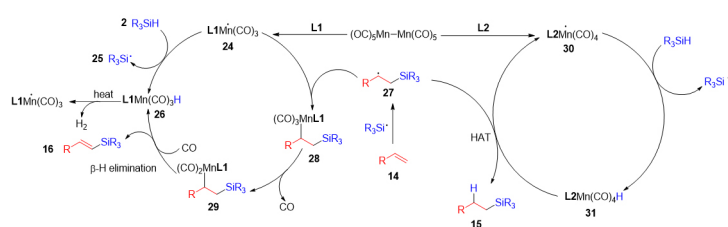
**Scheme 5.** Mn-catalyzed dehydrogenative silylation of alkenes to produce allylsilane. (A) Selected examples; (B) controlled experiments of deuterium labeling studies; and (C) linear alkene performance.

up to 99:1) (15-7 to 15-10).

After a thorough exploration of the mechanism, a reasonable mechanism for this ligand-tuned divergent silylation was described [Scheme 7]. Manganese radicals with different phosphine ligands were generated at



Scheme 6. Mn-catalyzed ligand-tuned divergent silylations of alkenes.



Scheme 7. The plausible reaction mechanism of ligand-tuned Mn-catalyzed dehydrosilylation and hydrosilylation of alkenes.

the beginning of the reaction. Both of these subsequently abstracted the H atom of silane, resulting in the formation of two corresponding Mn-H species ( $L1Mn(CO)_3H$  26,  $L2Mn(CO)_4H$  31). Concurrently, the co-generated silyl radical 25 rapidly added to the olefine, forming the uniform alkyl radical intermediate 27. In the dehydrosilylation circulation, the secondary alkyl radical 27 underwent a dynamically controlled radical coupling with the manganese radical 28; the generated alkyl manganese further had a CO dissociation, and a feasible  $\beta$ -H elimination delivered the terminal silylated alkene 16. When the manganese radical coordinated with electron-withdrawing JackiePhos, a direct HAT process with 27 occurred to provide the

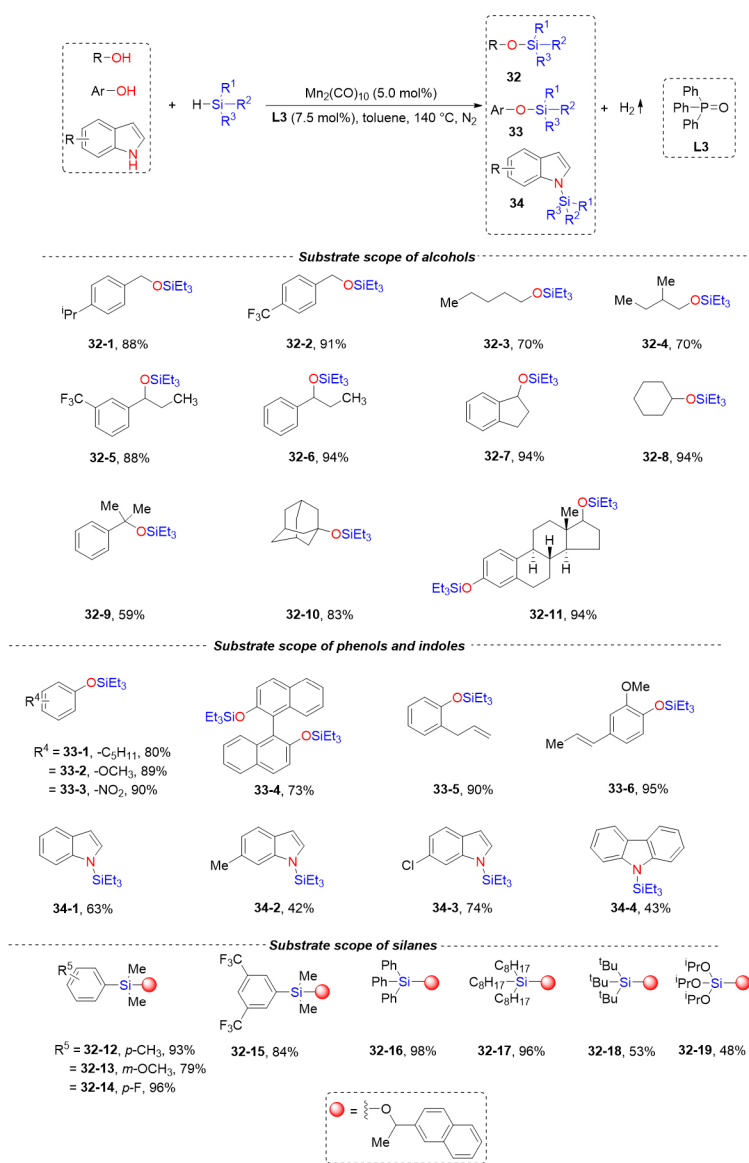
hydrosilylation products 15. The origin of ligand-tuned selectivity was also well-validated by DFT calculations.

Direct dehydrogenative coupling of silanes and hydroxyl compounds is ideal access to silyl ethers due to the high atom economy and practical utility. Hilal previously explored the dehydrogenative coupling of silanes with alcohols using a dinuclear manganese catalyst but obtained only moderate yields for methanol and ethanol. More recently, Li *et al.* employed commercially available phosphine oxide as a ligand for the dinuclear catalyst, enabling a practical and efficient dehydrogenative coupling between hydroxyl compounds and silanes [Scheme 8]<sup>[4]</sup>. In their protocol, primary (32-1 to 32-4), secondary (32-5 to 32-8), and even tertiary alcohols (32-9, 32-10) gave the desired silyl ethers in high yields. Phenols bearing different substituents, even with terminal and internal alkenes, were all tolerated in the Mn-catalyzed system (33-1 to 33-6). The scope of the catalytic system was expanded to include electron-poor indoles, where the NH group underwent dehydrogenative coupling, yielding N-silylation products (34-1 to 34-4). Furthermore, valuable silanols could be generated through dehydrogenative coupling using water as the coupling partner [Scheme 9]. Notably, the reaction scale of this dehydrogenative coupling could be amplified to 40 g without any loss of efficiency.

Radical capture experiments suggested that the common radical pathway initialized by  $\text{Mn}(\text{CO})_5\cdot$  in previous reports was not involved in the dehydrogenative coupling. According to a series of controlled experiments, an organometallic pathway was reasoned to explain the dehydrogenative coupling process [Scheme 10]. A feasible exchange of CO between phosphine oxide ligands occurred at the noted temperature, producing the actual catalyst 36 (Mn-I). The weak chelation between the soft metal center and the hard phosphine oxide ligand in 36 enabled an oxidative addition of Si-H to the active Mn atom. Then, the partner substrate with an acidic proton combined with the reactive H-Mn-Si species 37 (Mn-II), releasing one molecule of hydrogen (confirmed by GC) and the manganese species 38 (Mn-III). Finally, the spontaneous reductive elimination of 38 delivered the desired silylated products and regenerated 36.

In 2019, Liang *et al.* developed a visible-light-initiated manganese-catalyzed hydrosilylation of terminal and internal alkynes [Scheme 11]<sup>[37]</sup>. In the survey of carbonyl metal catalysts,  $\text{Mn}(\text{CO})_5\text{Br}$  gave a lower yield (40% yield) compared with  $\text{Mn}_2(\text{CO})_{10}$  (84% yield), which might be due to a higher BDE of Mn-Br (75 kcal/mol), but the binuclear iron complex ( $\text{Fe}_2\text{Cp}_2(\text{CO})_4$ ), which has a lower BDE of the Fe-Fe bond (28 kcal/mol), only gave trace silylated products. A range of valuable Z-vinylsilanes were provided in high yields under the catalysis of  $\text{Mn}_2(\text{CO})_{10}$  (up to 98% yield). The Ge-H bond was also successfully activated in the reaction conditions, and the phenylacetylene reacted with  $n\text{Bu}_3\text{GeH}$ , giving vinylgermanium with 97:3 Z/E selectivity. Deuterium-labeling experiments and radical inhibition experiments were conducted to propose a plausible mechanism. The  $\text{Mn}(\text{CO})_5$  radical arose from the visible-light-induced homolysis of the Mn-Mn bond, which abstracted the hydrogen atom from silanes. Silyl radical 40 was added to the triple bond, delivering the alkene radical intermediate 41 or 42. Finally, the desired Z-vinylsilane 4 was produced after the HAT process with  $\text{HMn}(\text{CO})_5$ .

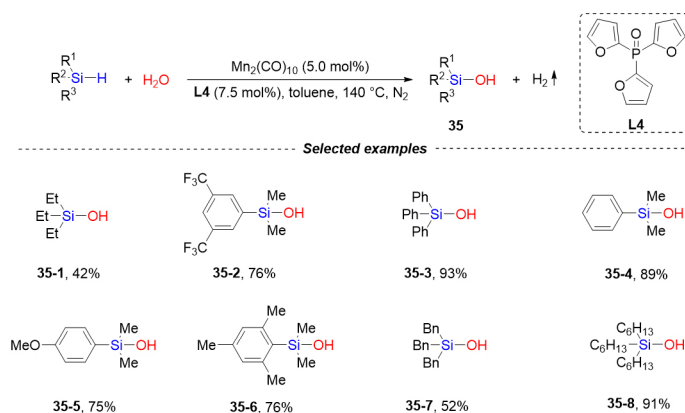
Vivien *et al.* reported a room-temperature manganese-catalyzed hydrosilylation of alkenes with 1,1,1,3,5,5,5-heptamethyltrisiloxane ( $\text{MD}^{\text{H}}\text{M}$ ) under UV irradiation [Scheme 12]<sup>[38]</sup>. The reaction did not proceed thermally and required UV irradiation for efficient hydrosilylation. A light “on/off” experiment demonstrated that the rate of hydrosilylation decreased drastically in the absence of UV irradiation. Different types of terminal alkenes were tolerated, but electron-deficient alkenes, such as *tert*-butylacrylate, did not yield any hydrosilylated products. Gem-alkenes and internal alkenes were not compatible with the Mn-catalytic system (15-11, 15-12); silanes were strictly limited to  $\text{MD}^{\text{H}}\text{M}$ , as only low-to-no conversions



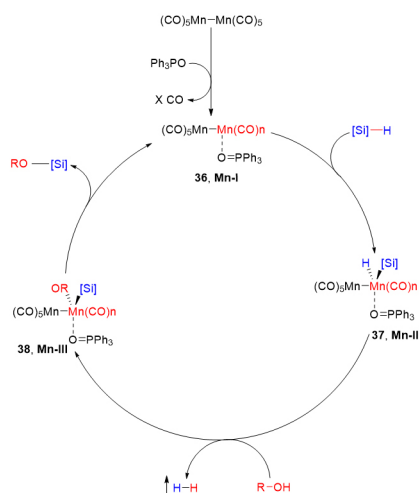
Scheme 8. The dehydrogenative coupling of alcohols, phenols, and indoles.

were observed when using other silane sources.

The direct reduction of carbonic acid and its derivate is an important access to aldehyde; Zheng *et al.* have focused on this area since 2012. They initially reported a UV-irradiation Mn-catalyzed hydrosilylation of carbonic acids synthesizing silylacetal [Scheme 13, Work A]<sup>[39]</sup>. The reactivity and chemoselectivity were determined by the choice of silane, with Et<sub>3</sub>SiH, PhMe<sub>2</sub>SiH, and Ph<sub>2</sub>MeSiH being reactive, while Ph<sub>3</sub>SiH was unreactive. Secondary silanes, such as Ph<sub>2</sub>SiH<sub>2</sub>, gave alcohol products because of over-reduction. After eight years, they upgraded the reaction system to perform ester reduction under visible-light irradiation [Scheme 13, Work B]<sup>[40]</sup>. Interestingly, ethyl esters were more reactive than methylated analogs (45-1, 45-2), and substituents on the benzylic group affected the reaction efficiency obviously (45-3, 45-4). Increased steric hindrance at the  $\alpha$ -position of the ester decreased reactivity (45-5), but the internal alkene could remain intact through the light-irradiation hydrosilylation (45-6). In both cases, the generated silylacetal



**Scheme 9.** The dehydrogenative coupling of water with different silanes.



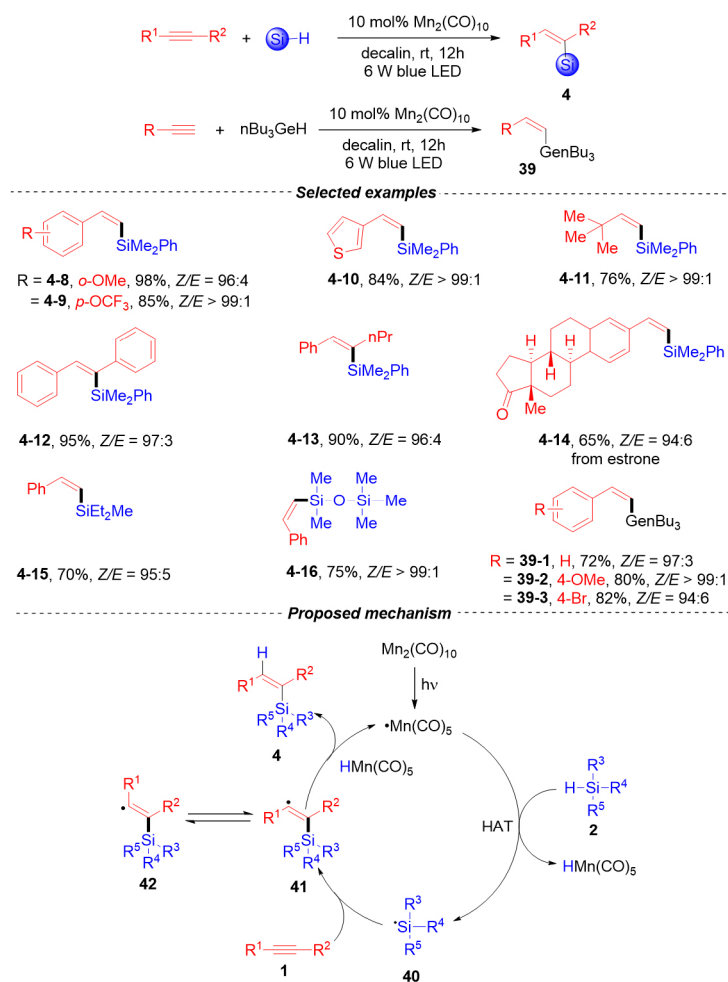
**Scheme 10.** The Organometallic dehydrogenative coupling between hydroxyl compounds and silanes controlled by phosphine oxide.

could undergo acidic hydrolysis, producing aldehydes smoothly.

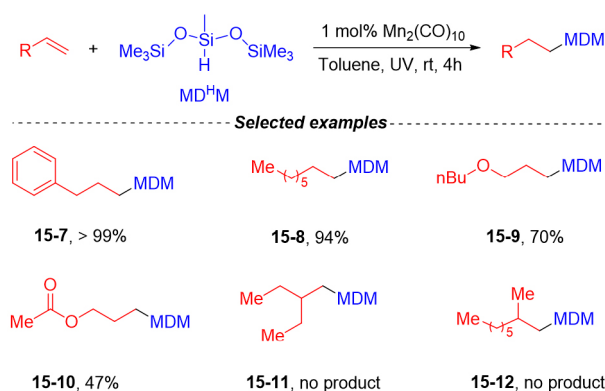
### Activation of C-X (F, Cl, I) bond

In 2005, Friestad reported a Mn-mediated alkyl addition of C=N via radical-addition pathway, stoichiometric  $\text{Mn}_2(\text{CO})_{10}$  was used to abstract the iodide-atom in RI generating the desired alkyl radical intermediate<sup>[26]</sup>. {Friestad, 2006 #1021; Friestad, 2006 #1202} Primary alkyl halides were more favored than secondary and tertiary alkyl halides, and good diastereoselectivity was obtained by adding excess equivalents of  $\text{InCl}_3$ . To demonstrate the practicability, (R)-coniine was smoothly synthesized from the addition product of 4-chlorobutyl radical with N-acylhydrazone after a four-step conversion [Scheme 14]<sup>[27]</sup>.

Although stoichiometric  $\text{Mn}_2(\text{CO})_{10}$  was necessary in Friestad's report, their finding really inspired other organic chemists to explore the possibility of  $\text{Mn}_2(\text{CO})_{10}$ -catalyzed ATR reactions. Building on this work, McMahon *et al.* reported an elegant carboacylation of alkenes with intramolecular alkyl iodides [Scheme 15]<sup>[19]</sup>. Only 2.5 mol% Mn-catalyst was devoted to the reaction, ensuring the I-atom transfer well under ambient light conditions. Through their reaction, not only five-membered rings but also six- and



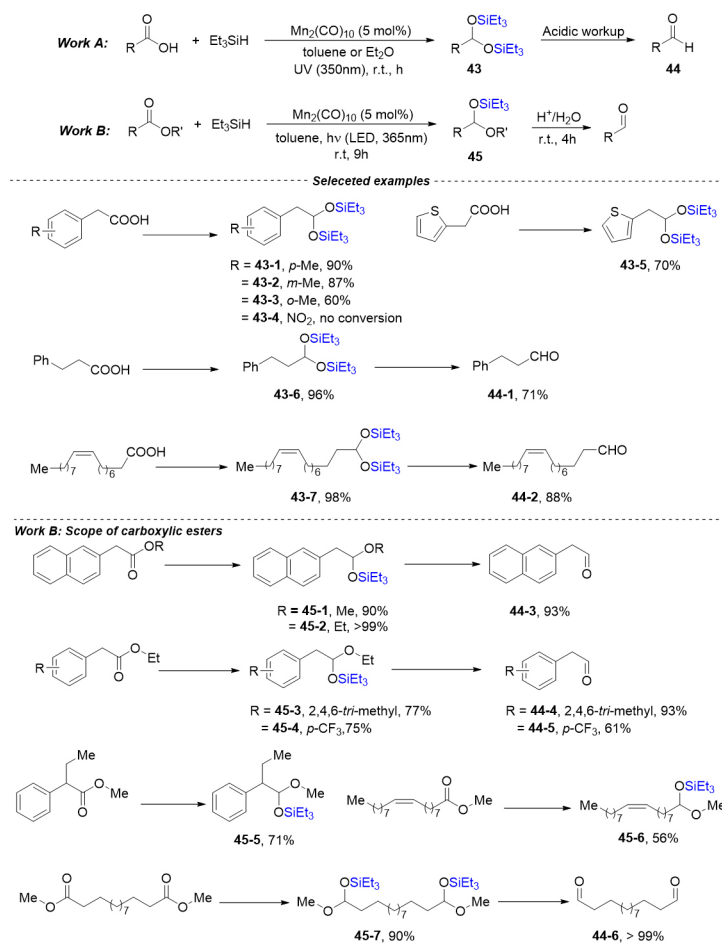
**Scheme 11.** Visible-light-initiated manganese catalyzed Z-Selective hydrosilylation and hydrogermylation of alkynes.



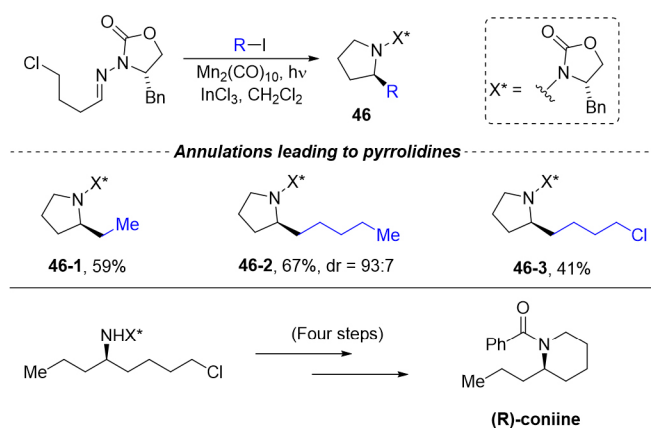
**Scheme 12.** Manganese-catalyzed hydrosilylation of various terminal alkenes with MD<sup>H</sup>M.

seven-membered rings were synthesized smoothly. Bicycle products were also obtained under optimized conditions. They proposed a reasonable mechanism for the Mn-catalyzed carboacylation. The I-atom in the substrate was abstracted by the active  $\cdot\text{Mn}(\text{CO})_5$ , delivering a carbon-centered radical. Subsequently,



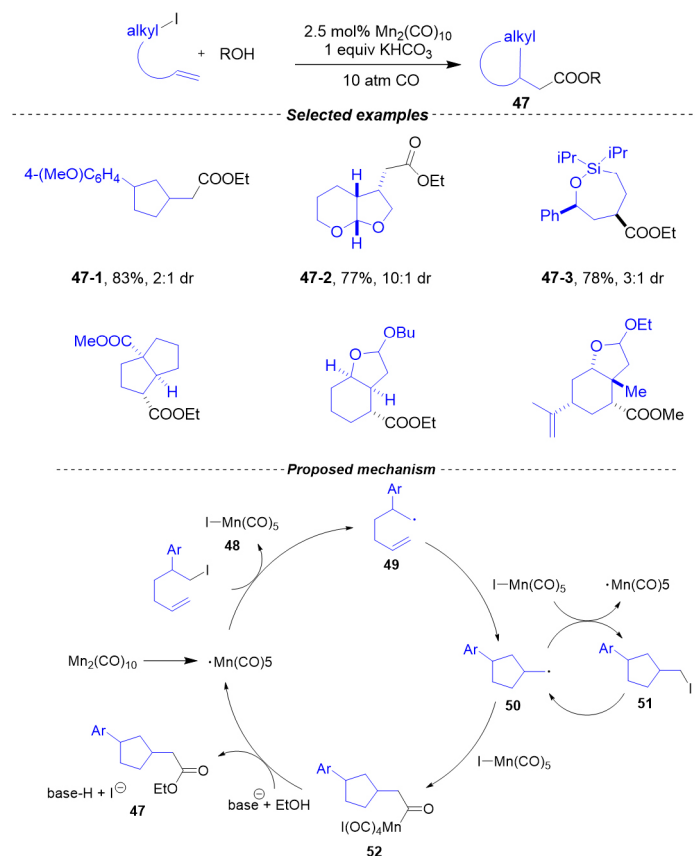


Scheme 13. Manganese-catalyzed selective reduction of acids and esters to aldehydes.



Scheme 14. Intermolecular alkyl radical addition to chiral N-acylhydrazones mediated by manganese carbonyl.

intramolecular alkene and carbonylation formed the acyl manganese 52 intermediate, which delivered the ultimate ester product after a feasible nucleophilic substitution. The cyclic alkyl-iodide 47, which was generated during the reaction, could also undergo another I-atom transfer process and give the desired

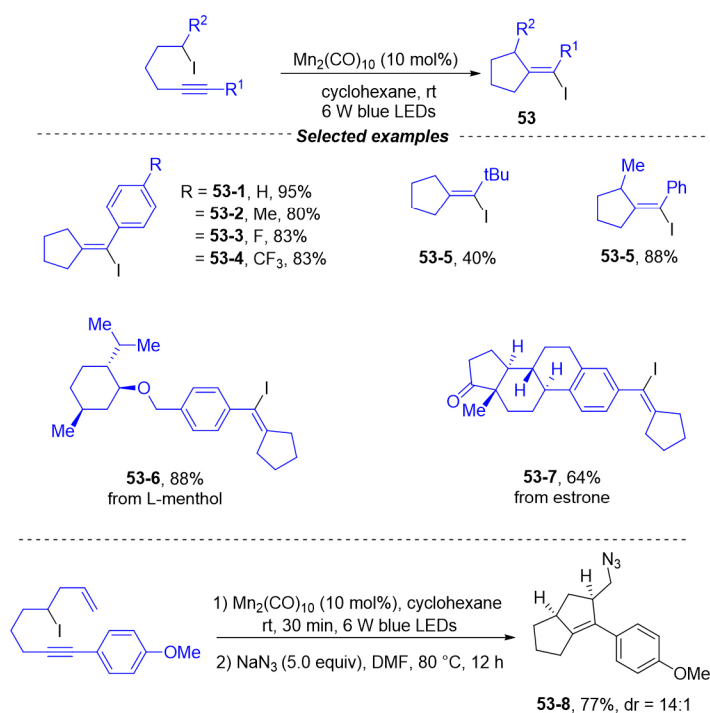


**Scheme 15.**  $\text{Mn}_2(\text{CO})_{10}$ -catalyzed carboacylation of alkenes with alkyl iodides.

carboacylation product.

Intrigued by McMahon's work, Weng *et al.* developed a Mn-photocatalyzed ATRC (atom transfer radical cyclization) of unactivated alkyl iodides [Scheme 16]<sup>[24]</sup>. A number of alkynyl iodides were efficiently transformed into alkenyl iodides in a short time (30 min). The reaction demonstrated good substrate tolerance, including complex-molecule-derived substrates. (53-6, from L-menthol 88% yield; 53-7, from estrone 64% yield). In the presence of an allyl group, a formal atom-transfer double radical cyclization occurred, leading to diquinane, an important structural motif in many natural products. It was noted that the reaction did not work in the dark, even at 120 °C, which further verified the photochemical nature of the transformation. Quantum yield ( $\Phi$ ), which was measured to be 1.5 ( $\lambda = 420 \text{ nm}$ ), indicated that a radical chain process rather than a closed catalytic cycle existed in the radical cyclization.

The introduction of fluoroalkyl groups into bioorganic molecules can effectively enhance their lipophilicity, metabolic stability, and biological activity. Visible-light-mediated atom transfer radical addition (ATRA) of fluoroalkyl halides to alkenes or alkynes is one of the most direct and atom-economical methods. Based on their previous work in Mn-catalyzed ATRs, Ji *et al.* explored the iodofluoroalkylation of alkynes and alkenes using dimeric manganese under blue-light irradiation [Scheme 17]<sup>[41]</sup>. The desired iodofluoroalkylated product was successfully isolated in 71% yield with 96:4 E/Z selectivity when the reaction was carried out in  $\text{CH}_2\text{Cl}_2$  under blue-light irradiation. After an optimization of reaction conditions, a broad scope of alkynes bearing different functional groups was investigated and gave E-fluoroalkylated alkenyl iodides in high

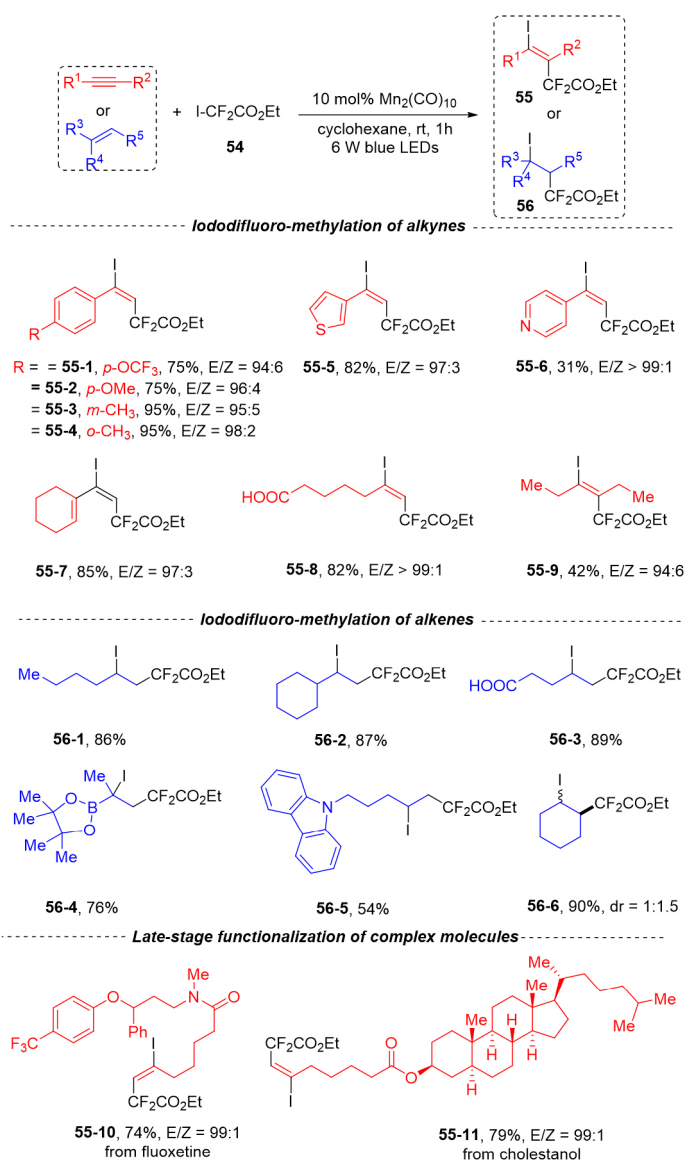


**Scheme 16.** Visible-light-promoted manganese-catalyzed atom transfer radical cyclization of unactivated alkyl iodides.

yields and chemoselectivities (up to 95% yield, up to 99:1 E/Z), and double bond was also difunctionalized smoothly under the optimized conditions.

A similar reaction mechanism existed in the two atom-transfer reactions, but here, we only discuss the latter one [Scheme 18]. As in previous examples, the active  $\text{Mn}(\text{CO})_5$  radical, generated through the homolysis of the Mn-Mn bond, abstracted the iodine atom from perfluoroalkyl iodides, resulting in the formation of  $\text{Mn}(\text{CO})_5\text{-I}$  and the fluoroalkyl radical 57. The vinyl radical intermediate 58 was then generated after a radical addition of  $\text{R}_f^\bullet$  to an unsaturated bond. The vinyl radical could absorb the iodine atom from perfluoroalkyl iodide substrates or from  $\text{Mn}(\text{CO})_5\text{-I}$ , giving the difunctionalized product. The high *E*-selectivity during the I-atom transfer was attributed to the electrostatic repulsion between the  $\text{R}_f$  group in vinyl radical intermediate (58) and  $\text{R}_f\text{-I}$  or  $\text{Mn}(\text{CO})_5\text{-I}$ . Considering the lower BDE and the high concentration of  $\text{R}_f\text{-I}$ , the author reasoned that *path a* was likely the major reaction pathway.

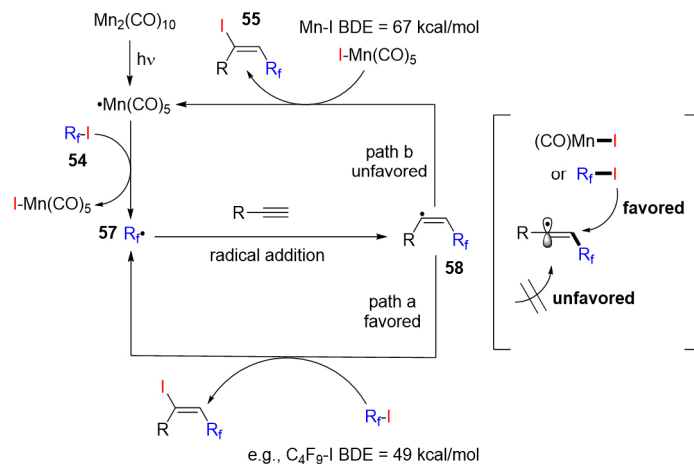
Visible-light-mediated Minisci reaction is a mild and effective method for the C-H alkylation of heteroarenes. Nuhant *et al.* disclosed a mild and robust method that was a photoredox Minisci reaction of unactivated iodoalkanes with heteroarenes catalyzed by  $\text{Mn}_2(\text{CO})_{10}$  [Scheme 19]<sup>[22]</sup>. Primary (61-1, 61-2), secondary (61-3, 61-4), and tertiary (61-5, 61-6) iodoalkanes, including even acid-sensitive groups such as oxetane, sugar moiety, azetidine, and tert-butyl carbamate, were well tolerated in this protocol. The scope of other heterocyclic substrates was examined under the model conditions as also displaced (61-7, 61-8). Additionally, alcohols pretreated with iodo-Ghosez's reagent could also serve as another effective source of the alkyl radical (61-5, 61-6, 61-9 to 61-11), which could reduce the reaction cost, especially in large-scale production. Moreover, the late-stage C-H alkylation of peptides and biotin occurred smoothly, making it useful for labeling and bioconjugation of reactive heteroaromatic molecules (61-12, 61-13).



**Scheme 17.** Manganese-mediated iododifluoro-methylation of alkynes and alkenes.

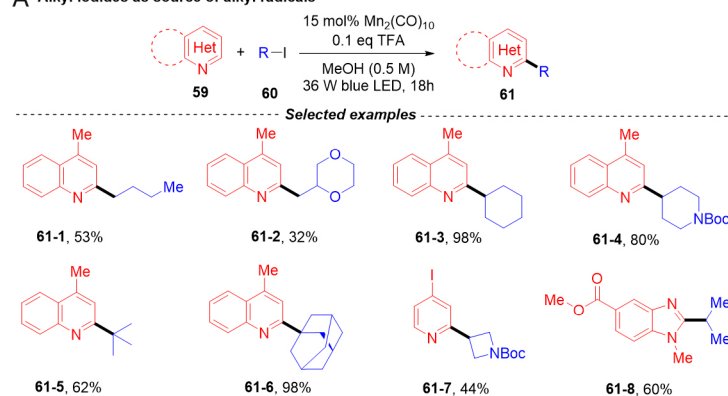
With the support of DFT calculations, a reasonable reaction mechanism was proposed [Scheme 20]. Similar to previous examples of the Mn-catalyzed atom-transfer-reaction, the reaction was started with the activation of the R-I bond by the free  $\text{Mn}(\text{CO})_5$  radical. Subsequently, a radical addition occurred between the nucleophilic alkyl radical and the protonic heteroaromatic ring. A following deprotonation assisted by  $\text{CF}_3\text{COO}^-$  delivering the alpha-amino alkyl radical 64. The generated radical intermediate 64 could be oxidized to the final alkylated product 61 via a single electron transfer (SET) process with  $\text{I-Mn}(\text{CO})_5$  or  $\text{Mn}_2(\text{CO})_{10}$ .

Giese reactions using alkyl iodides that form  $\text{C}(\text{sp}^3)\text{-C}(\text{sp}^3)$  bonds facilitated by traceless activation groups are a useful addition to the medicinal chemistry toolbox. Dong *et al.* reported a visible-light-initiated  $\text{Mn}_2(\text{CO})_{10}$ -catalyzed Giese addition reaction, which is independent of the reduction potential of the photoredox catalyst [Scheme 21]<sup>[42]</sup>. In their reaction, Hantzsch ester was applied as the hydrogen source. The steric and

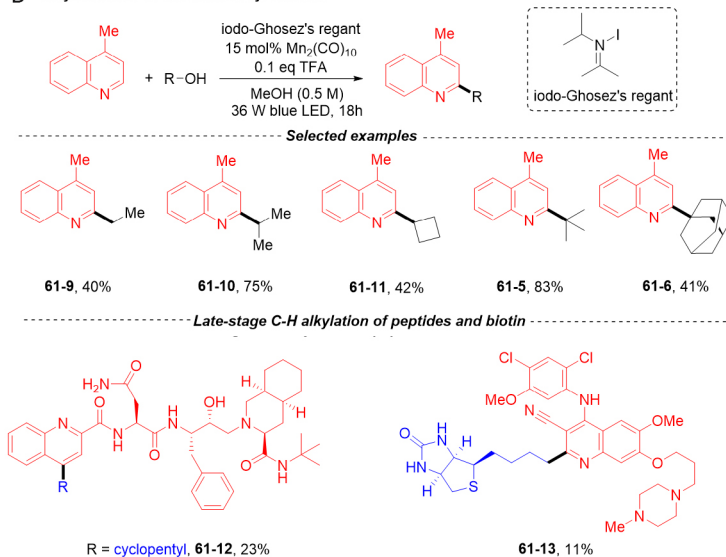


**Scheme 18.** The plausible reaction mechanism of iododifluoro-methylation.

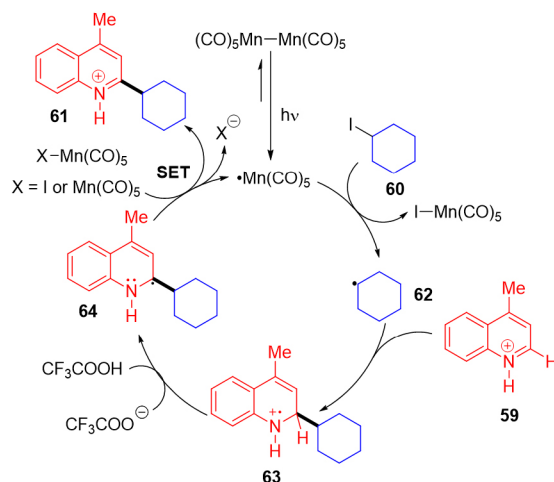
**A** Alkyl iodides as source of alkyl radicals



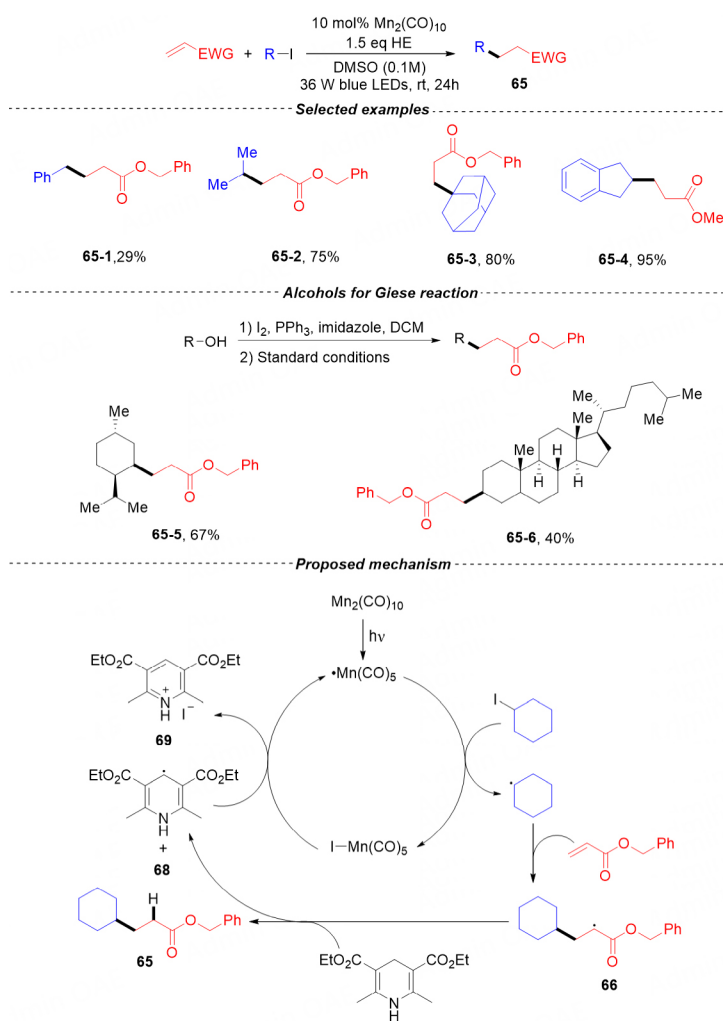
**B** Alkyl alcohols as source of alkyl radicals



**Scheme 19.** The C-H alkylation of heterocycles using alkyl iodides or alkyl alcohols as alkyl radical sources.



Scheme 20. The plausible reaction mechanism of visible-light-driven Minsic reaction.



Scheme 21. Visible-light-mediated Giese reaction to form C-C bonds.

electronic factors of the alkyl iodide substrates had little effect on the efficiency, except for benzyl iodide, which showed a low yield (65-1, 29%). Alkyl bromides and alkyl chlorides exhibited no reactivities under the Mn-catalysis. Alcohols could be the precursors of alkyl iodides in the presence of molecular iodide, providing the same products smoothly (65-5, 65-6). After a series of mechanism explorations, they proposed a reaction mechanism based on experiment results and previous literature. The Mn-Mn bond was homolyzed to the reactive manganese radical  $\text{Mn}(\text{CO})_5\cdot$  under light-irradiation, then an iodine abstraction occurred between the metal radical and alkyl iodides, giving the alkyl radical. A radical addition with alkene constructed the desired C-C bond, and reduction with Hantzsch ester gave the ultimate product and regenerated the reactive manganese radical.

After this work, the same group used a similar strategy, realizing allylation reactions between unactivated alkyl iodides and allyl sulfones [Scheme 22]<sup>[43]</sup>.

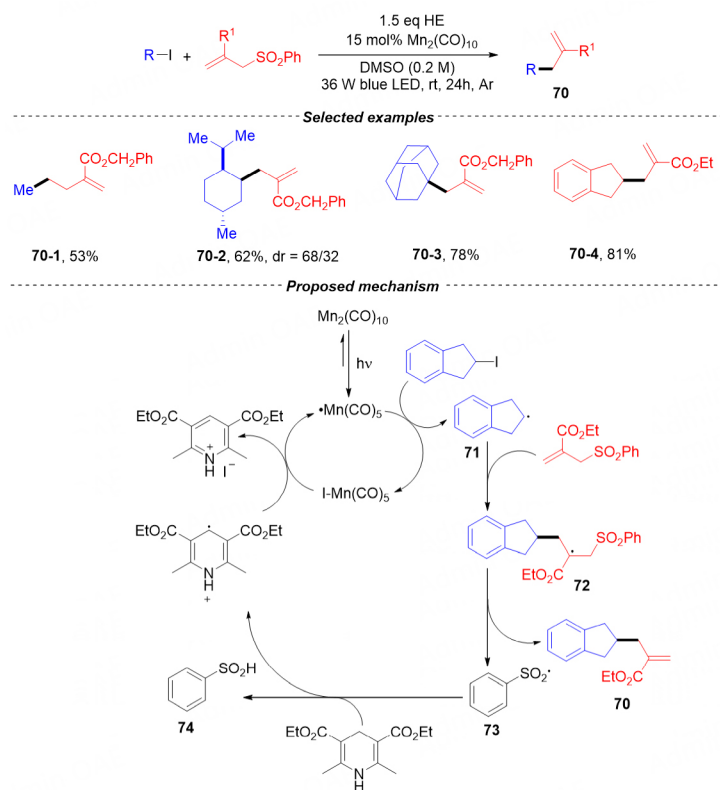
With their consistent interests in the area of light-irradiation Mn-catalyzed radical alkylation. Wang *et al.* further explored the application of the combination of  $\text{Mn}_2(\text{CO})_{10}$  and Hantzsch ester in other organic reactions. They utilized  $\text{Mn}_2(\text{CO})_{10}$  in a three-component reaction of imine (generated in situ by condensation of benzaldehydes and anilines) and alkyl iodides to synthesize secondary amines [Scheme 23]<sup>[44]</sup>. This transformation required a catalytic amount of AcOH to promote the condensation of aldehydes and amines. This three-component reaction had a broad substrate scope, tolerating different substituted aryl aldehydes and anilines, as well as primary, secondary, and tertiary alkyl iodides.

Gem-difluoroalkenes have attracted extensive attention because they are not only important building blocks in organic synthesis but also play crucial roles in pharmacologically active molecules and drug efficacy. However, a practical large-scale synthesis method for this important molecule remains elusive. Guo *et al.* achieved the preparation of gem-difluoroalkenes through a relay-catalysis strategy using a combination of  $\text{Mn}_2(\text{CO})_{10}$  and an iridium-based photocatalyst [Scheme 24]<sup>[45]</sup>. Screening of various photocatalysts revealed that  $[\text{Ir}(\text{dF}(\text{CF}_3)\text{ppy})_2(\text{dtbbpy})]\text{PF}_6$  was the most suitable. The presence of a base, such as  $\text{K}_2\text{HPO}_4$ , was found to be crucial for the reaction efficiency. Primary iodoalkanes containing TMS,  $\text{CF}_3$ , and *p*-methoxybenzyl groups afforded the target products in moderate yields.  $\text{Csp}^3\text{-I}$  was the most reactive bond compared to other C-halogen bonds. Substituents on  $\alpha$ -trifluoromethyl alkenes affected the reaction negligibly, and heteroaryl-substituted  $\alpha$ -trifluoromethyl alkenes were also compatible.

In the proposed mechanism [Scheme 25], the Mn-catalyzed cycle followed a similar pathway to their previous work, involving the generation of the desired alkyl radical and Mn-I species through an iodine-transfer reaction. The alkyl radical was then added to  $\alpha$ -trifluoromethyl alkene, generating radical **78**. Meanwhile, photoexcited  $[\text{Ir}(\text{dF}(\text{CF}_3)\text{ppy})_2(\text{dtbbpy})]\text{PF}_6$  underwent a SET process and was quenched by HE to form  $\text{Ir}^{\text{II}}$  species and radical species **81**.  $\text{Ir}^{\text{II}}$  then reduced radical species **78**, resulting in the formation of a  $\text{CF}_3$ -styrene carbanion intermediate **79** while simultaneously regenerating the  $\text{Ir}^{\text{III}}$  photocatalyst. Finally, a base-promoted  $\beta$ -fluoride elimination of the carbanion afforded the final gem-difluoroalkene **77**. The Mn-I species was reduced to active Mn radical by the deprotonated **82**, completing the catalytic cycle.

The ketyl radical is a kind of highly reactive C-centered radical that complements the classic, polar C-C bond construction well. However, the generation of this type of radical relies on extremely strong reductants, such as Na and K, which limit the development of ketyl radical chemistry heavily. In 2018, Wang *et al.* pioneered an excellent Mn-catalyzed radical halogen-atom transfer process to obtain ketyl radical instead of classic carbonyl reduction [Scheme 26]<sup>[20]</sup>. In their state-of-art, the radical  $\text{Mn}(\text{CO})_5\cdot$  abstracted  $\text{I}\cdot$  from the in-situ generated  $\alpha$ -acetoxy iodide **85** affording the ketyl radical **88**, then it further

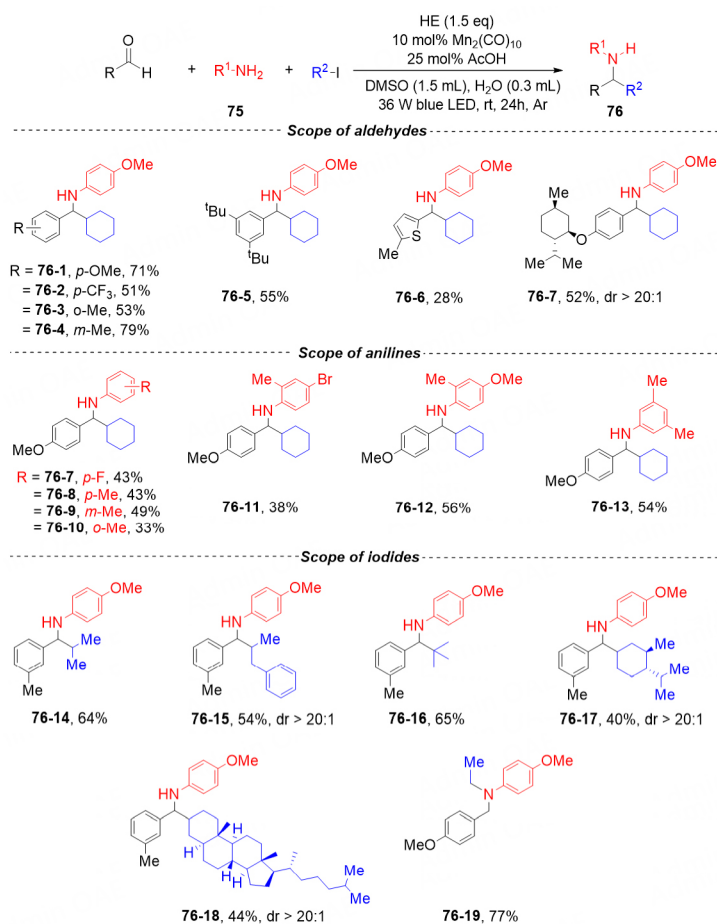




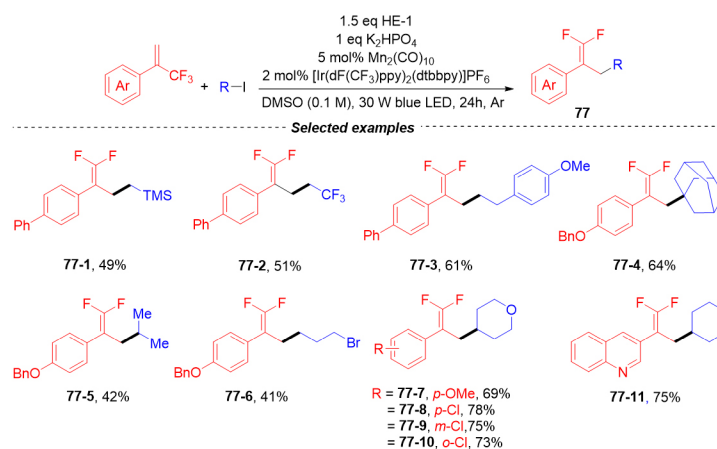
**Scheme 22.** Visible-light-mediated allylation reactions between unactivated alkyl iodides and allyl sulfones.

coupled with alkyne substrate producing a vinyl radical 89. Under Mn-catalyzed conditions, the vinyl radical would not occur a single-electron-reduction to form the allyl ester product 92 but was subsequently oxidized by Mn-I species, giving the ultimate vinyl iodide 84. After a careful exploration of the origin of the high *Z:E* diastereoselectivity, the author found that a longer reaction time could enhance the *Z:E* ratio of products. With the optimized conditions in hand, alkynes with different functional groups containing SiEt<sub>3</sub>, BPin, and electron-deficient propiolates underwent ketyl coupling feasibly. A wide range of aliphatic aldehydes with both small and large steric footprints provided the corresponding *Z*-vinyl iodides smoothly in high *Z:E* selectivities. Furthermore, Rafferty *et al.* reported a cross-selective aza-pinacol coupling with ketyl radical and imine via the Mn-catalyzed atom transfer reaction [Scheme 27]<sup>[21]</sup>. Their protocol avoided the formation of imine-derived homodimers typically observed in previous reports. During the reaction optimization, the authors found that white CFL gave a higher yield than blue LED; the combination of Zn and Cy<sub>2</sub>NEt significantly facilitated the cross-coupling. A range of 1,2-amino alcohols was delivered in moderate to high yields (50%-92% yields) but with low diastereoselectivities (1:1 to 10:1). When *S*-aryl sulfinimines were devoted to the reaction, chiral 1,2-amine alcohol was obtained in 98% *ee* after oxidation of the cross-coupling products (94-9). In the mechanism exploration, they found that the [Mn]-I-NR<sub>2</sub> EDA complex facilitated milder reductive turnover of the Mn catalyst, which determined the occurrence of the radical cross-coupling.

Although Mn-catalyzed atom transfer reactions with aliphatic iodides have been intensively explored since the 2010s, transformations with aliphatic bromides which possess lower reactivity (BDE of the C-Br bond ≈ 69 kcal mol<sup>-1</sup> vs. BDE of the C-I bond ≈ 57 kcal mol<sup>-1</sup>) was still rarely established. Xie *et al.* realized a Mn<sub>2</sub>(CO)<sub>10</sub>-catalyzed divergent silylation of alkenes through a ligand-tuning strategy and wondered if the atom-

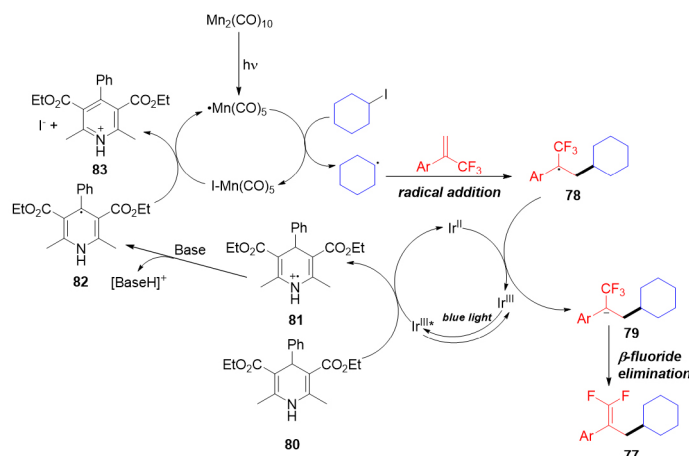


**Scheme 23.** Manganese-catalyzed three-component reaction of unactivated alkyl iodide, aniline, and aldehyde.

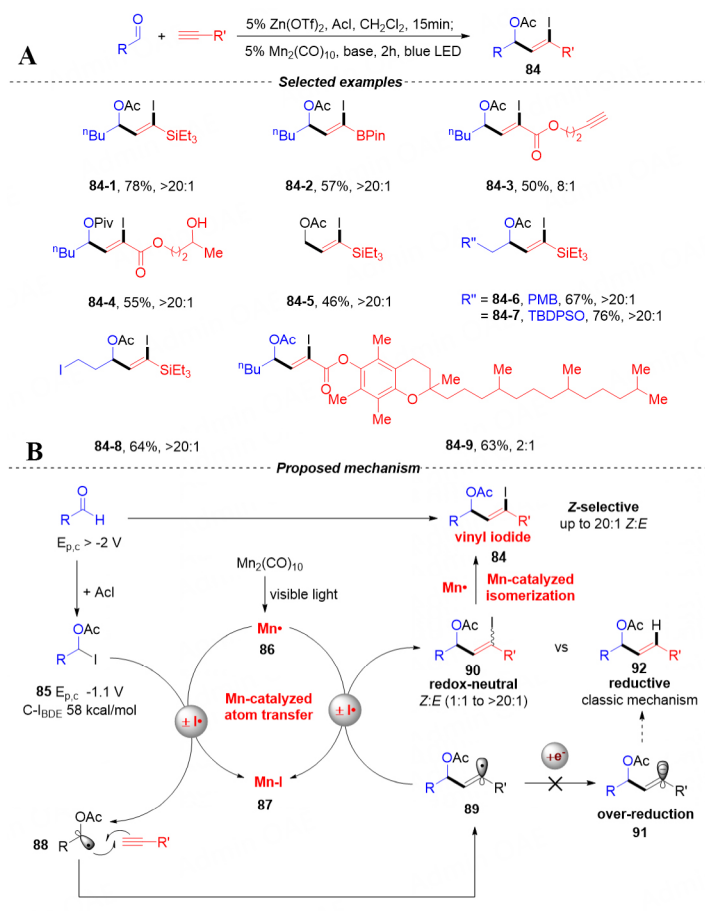


**Scheme 24.** The substrate scope of alkyl iodides and  $\alpha$ -trifluoromethyl alkenes.

transfer capability of Mn radicals could also be improved with a suitable ligand. Very recently, they reported a manganese-catalyzed light-mediated hydrofluoroalkylation of alkenes with fluoroalkyl bromides promoted by a bidentate phosphine ligand [Scheme 28]<sup>[25]</sup>. Among the screened phosphine ligands, a simple

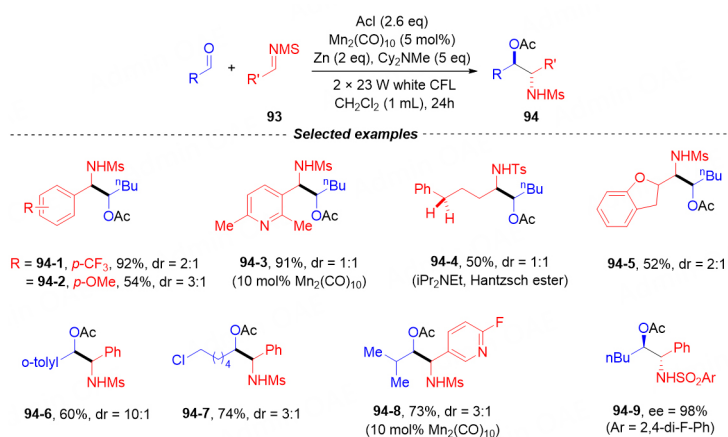


**Scheme 25.** The plausible reaction mechanism of photoredox relay-catalyzed gem-difluoroallylation of alkyl iodides.



**Scheme 26.** (A) Redox-neutral ketyl radical coupling; (B) The plausible reaction mechanism.

and commercially available bidentate phosphine (L5) exhibited superior catalytic activity; the desired hydrofluoroalkylated product was isolated in 84% yield. They conducted a comprehensive substrate investigation and found that more than 80 alkenes gave the corresponding products in satisfactory yields.



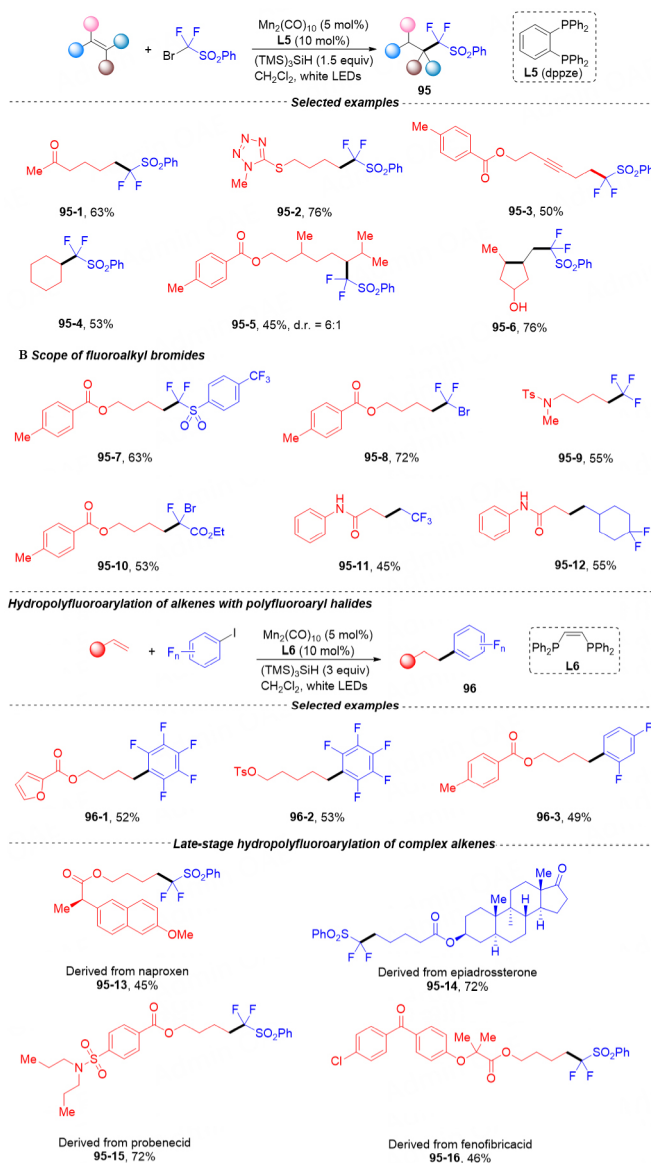
**Scheme 27.** Cross-selective aza-pinacol coupling via atom transfer catalysis.

Diffuoroalkyl, difluoromethyl, trifluoromethyl, monofluoroalkyl, and polyfluoroalkyl bromides were all tested under the model condition and were all workable. Hydropolyfluoroarylation of alkenes with  $\text{Ar}_F\text{-I}$  was also reliable in the Mn-catalytic system when L5 was instead by L6. Controlled experiments and DFT calculations indicated that the added phosphine ligand not only reduced the energy barrier during the bromide-transfer processes but also increased the stability and lifetime of the manganese radical.

Liu *et al.* developed a simple and efficient protocol to generate amidyl radicals from amine functionalities through a manganese-mediated ATR. In their envision,  $\text{Mn}_2(\text{CO})_{10}$  was used as the catalyst to activate the N-Cl bond in the in-situ generated N-chlorosulfonamide generating the desired N-centered radical intermediate for novel radical cascade reactions [Scheme 29]<sup>[23]</sup>. They successfully achieved site-selective chlorination of  $\text{C}(\text{sp}^3)\text{-H}$  bonds using this strategy. By using alkylamine-derived sulfonamides as model substrates and TCCA (trichloroisocyanuric acid) as the electrophilic chlorinating reagent, they were able to isolate the desired  $\delta\text{-C}(\text{sp}^3)\text{-H}$  chlorinated product in good yield (40% yield). After employing *t*BuOCl as the Cl-atom source, the C-chain chlorinated product was obtained in 80% yield. Under the optimized conditions, the alkyl chain in various sulfonamides and carboxamides was smoothly chlorinated with moderate efficiencies and excellent  $\delta$ -site selectivity. The success of this manganese-mediated atom transfer strategy to the intramolecular and intermolecular chloroamination of alkenes demonstrated the utilization value well in organic synthesis.

A plausible reaction route was proposed according to a series of mechanism-exploring experiments and DFT calculations [Scheme 30]. Firstly, the NH group was chlorinated by the electrophilic chlorinating reagent affording N-Cl amide **100**, then the highly active  $\text{Mn}(\text{CO})_5$  radical abstracted the Cl-atom from **101**, giving the amidyl radical **102**, after a thermodynamically favored 1,5-hydrogen atom-transfer, the C-radical species **103** was delivered smoothly. Then, the Cl-atom transfer proceeded through two possible pathways. Although DFT calculations pointed out that the Cl-atom in the product was from N-Cl amide rather than  $\text{Mn}(\text{CO})_5\text{Cl}$  due to the higher free energy activation barrier, the author did not preclude the possibility of path b.

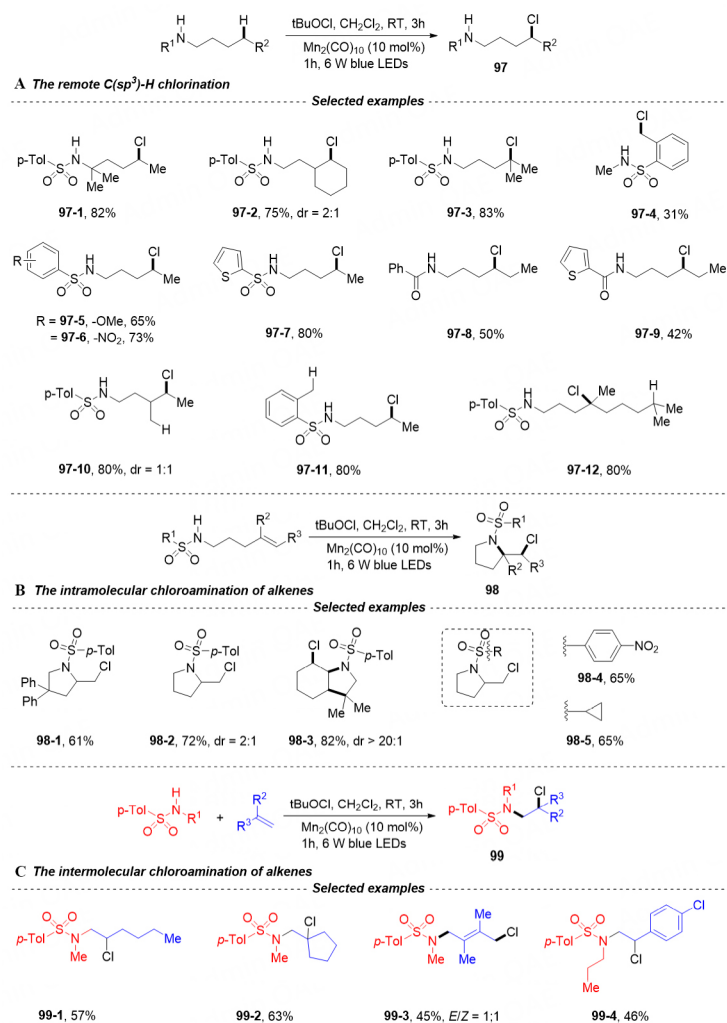
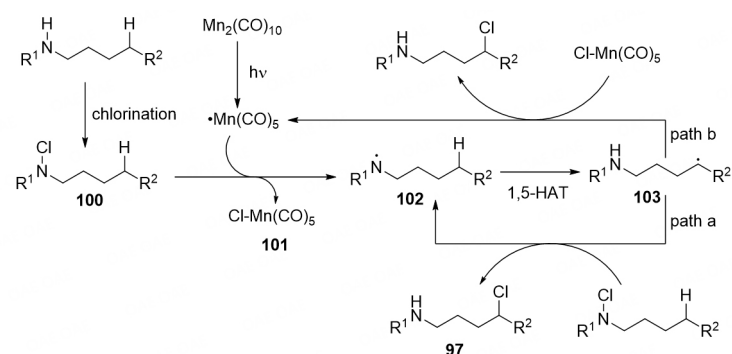
In a subsequent study, Ji *et al.* extended their manganese-catalyzed atom-transfer strategy to activate the N-F bond in N-fluorosulfonamides. This allowed for intramolecular/intermolecular hydroaminations of alkenes, two-component carboamination of alkenes, and even three-component carboamination of alkenes at room temperature [Scheme 31]<sup>[28]</sup>. The presence of  $(\text{EtO})_3\text{SiH}$  was crucial for the N-F bond activation, as



**Scheme 28.** Photoinduced manganese-catalyzed hydrofluorocarbonylation of alkenes.

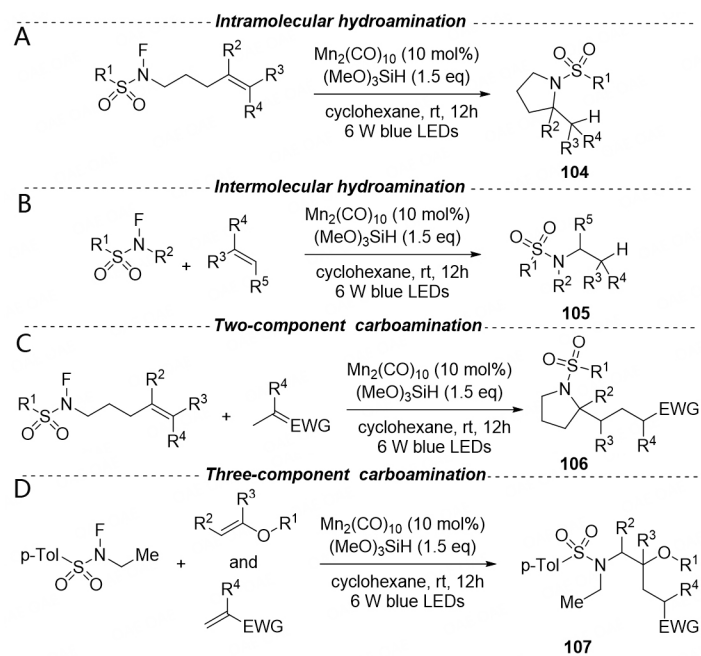
it facilitated the capture of the F-atom by a silyl radical, which was clearly observed by GC-MS.

Just a few months ago, Li *et al.* described a method for the unprecedented visible light irradiated manganese-catalyzed hydrosulfonylation of alkenes using sulfonyl chlorides [Scheme 32]<sup>[46]</sup>. This represented the first example of hydrosulfonylation of alkenes mediated by a manganese catalyst. By employing  $Mn_2(CO)_{10}$  and a (diphenylphosphanyl)propane ligand, they achieved the selective sulfonation of a variety of alkenes with sulfonyl chlorides, delivering the corresponding products in high yields (72% yield). Various alkenes and sulfonyl chlorides were tolerated well in the reaction, and a diverse array of substrates derived from drugs, such as isoxepac and estrone, could be readily modified to deliver the corresponding products in high yields.

Scheme 29. Manganese-catalyzed remote C(sp<sup>3</sup>)-H chlorination.

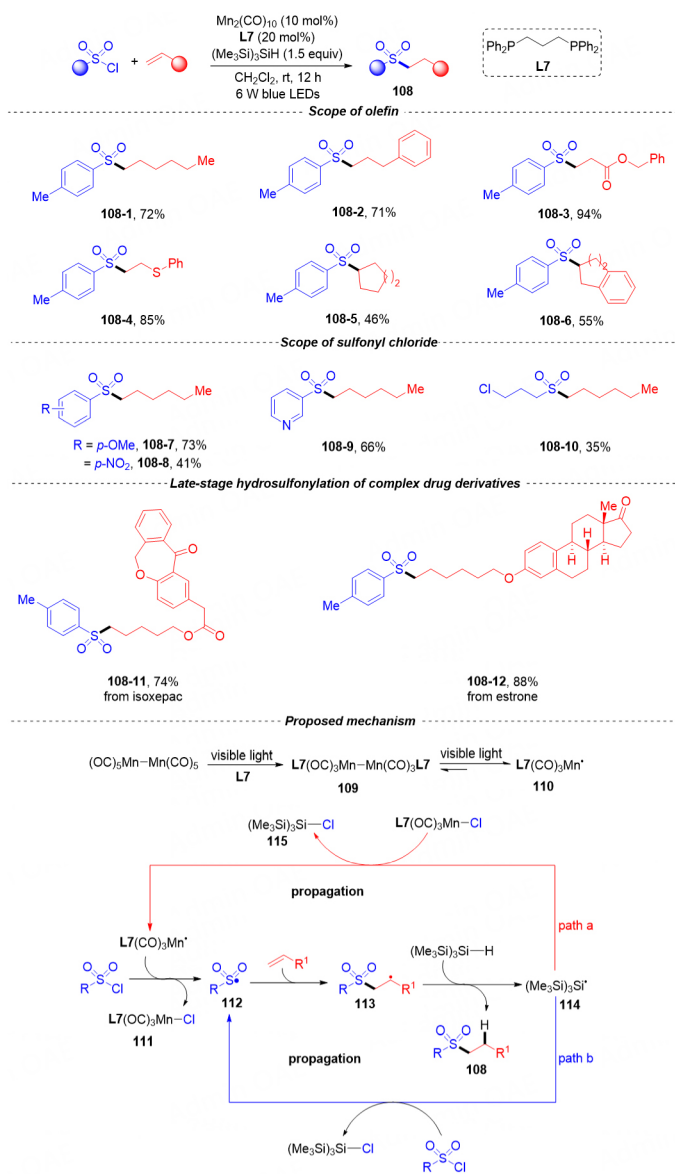
Scheme 30. The plausible reaction mechanism.

As early as the 1970s, Mach *et al.* found that the homolysis of  $\text{Mn}_2(\text{CO})_{10}$  under air atmosphere could deliver an unstable peroxy radical  $\text{Mn}(\text{CO})_5\text{OO}\cdot$ . However, the application of this manganese peroxy radical seemed to be ignored by researchers<sup>[29]</sup>. Until recently, Meng *et al.* found that the highly reactive metallic



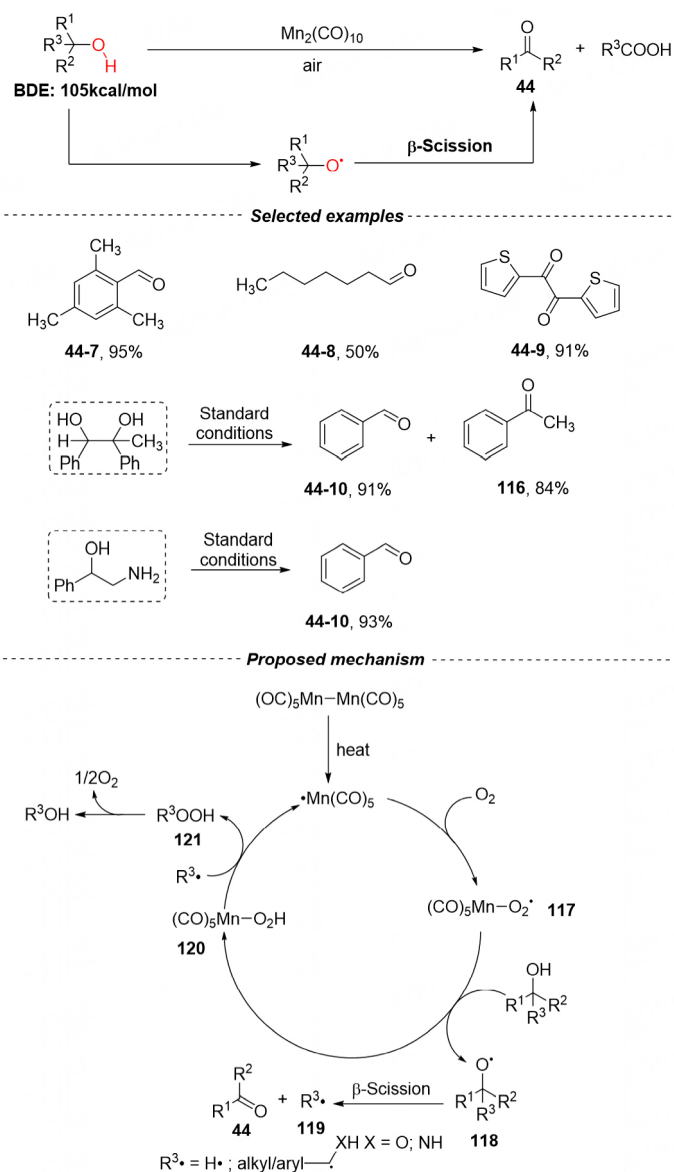
**Scheme 31.** (A) Intramolecular hydroaminations; (B) intermolecular hydroaminations; (C) two-component carboamination; and (D) three-component carboamination of alkenes.





**Scheme 32.** Visible light-initiated  $\text{Mn}_2(\text{CO})_{10}$ -catalyzed hydrosulfonylation of alkenes.

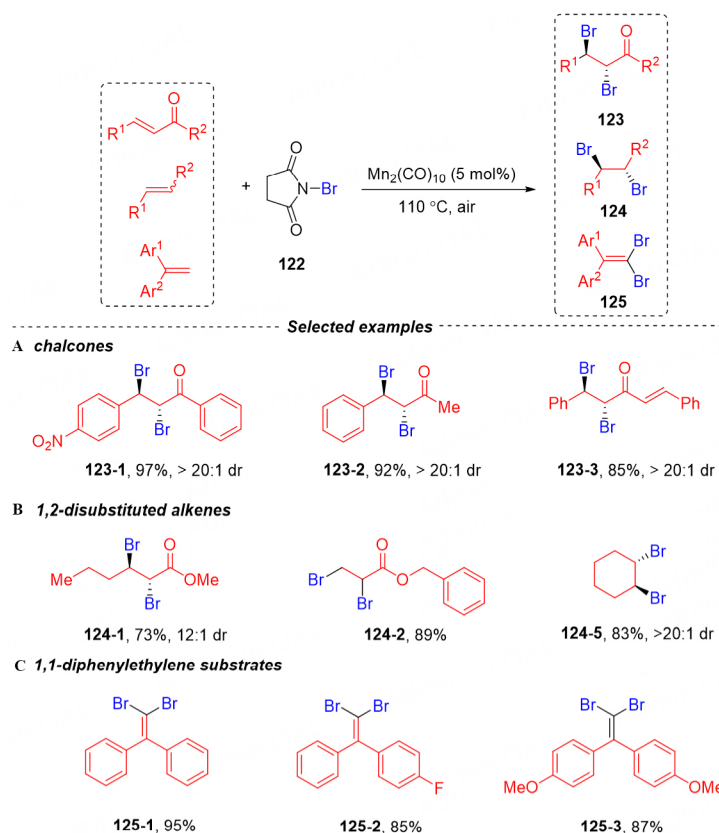
peroxy-radical could be used for the single-electron oxidation of hydroxyl groups, enabling the chemoselective oxidation of alcohols using air as the ultimate oxidant [Scheme 33]<sup>[31]</sup>. Under optimized conditions, benzylic alcohols were smoothly oxidized to the corresponding carbonyl products in high yields, while aliphatic alcohols delivered the corresponding aldehydes with lower yields. To further expand the application of this Mn-catalyzed oxidation, the oxidation-cleavage of 1,2-diols and 1,2-amino alcohols was also tried, and corresponding aldehyde or ketone products were both isolated in high yields. In the mechanism exploration, EPR signals showed that  $\text{Mn}(\text{CO})_5\text{OO}\cdot$  exactly existed in the oxidation, and the <sup>18</sup>O-labeled experiment indicated that there was no re-bound process. Based on these results and other controlled experiments, a novel oxidation mechanism via alkoxy radical intermediates was proposed [Scheme 32]. The real-active  $\text{Mn}(\text{CO})_5-\text{O}_2\cdot$  peroxy radical 117 was generated feasibly when  $\text{Mn}_2(\text{CO})_{10}$  was heated under air atmosphere, then it subsequently oxidized the hydroxyl group of alcohol substrate to the corresponding alkoxy radical 118, an intramolecular  $\beta$ -scission of 118 occurred rapidly, delivering the



**Scheme 33.** Selective oxidation of alcohols catalyzed by  $\text{Mn}_2(\text{CO})_{10}$ .

carbonyl products **44** and alkyl or hydrogen radical **119**. Then, manganese peroxide **120** was reduced by this free radical and regenerated  $\text{Mn}(\text{CO})_5\cdot$ .

After the oxidation of alcohols, Song *et al.* explored the Mn-catalyzed oxidation in the direct dibromination of alkenes using N-bromo-succinimide (NBS) as the bromine source [Scheme 34]<sup>[32]</sup>. When the dibromination was first tried with chalcone as the substrate, the desired product was isolated in a promising yield (16% yield) with high *dr* (14:1). After a quick optimization of solvents, the 1,2-dibrominated ketone was isolated in 91% yield with 18:1 *dr*. A broad range of substituted chalcones and 1,2-disubstituted alkenes were investigated in this protocol, and all gave the dibromination products high yields and excellent diastereoselectivity. For 1,1-diphenylethylenes, it was found that brominated-substitution took place at the terminal carbon atom instead of Br-atom addition; mono- or di-bromination could be controlled by the usage of NBS. Controlled experiments showed that  $\text{O}_2$  was necessary for this reaction, which suggested the



**Scheme 34.** Dibrominated addition and substitution of alkenes catalyzed by  $\text{Mn}_2(\text{CO})_{10}$ .

reaction pathway was different from previous Mn-mediated ATRs.

## CONCLUSION AND OUTLOOK

From the above reviews, it can be seen that the binuclear manganese catalyst  $\text{Mn}_2(\text{CO})_{10}$  has been intensively explored for diverse organic transformations, such as hydrosilylation and dehydrosilylation of unsaturated bonds, the construction of C-C bonds, alcohol oxidation, and so on. In most of these elegant precedents, the cleavage of the Mn-Mn bond generating  $\text{Mn}(\text{CO})_5$  radical is a universal beginning of the reactions, and a radical atom-transfer process with silanes and halide compounds promises the occurrence of desired reactions. However, the  $\text{Mn}_2(\text{CO})_{10}$ -mediated other types of reaction processes have rarely been reported, and the co-catalysis with other catalytic systems is still underdeveloped. To our knowledge, the application of  $\text{Mn}_2(\text{CO})_{10}$  in unsymmetric catalysis has never been disclosed. Therefore, we hope more novel organic transformations will be realized through the di-manganese catalysis.

## DECLARATIONS

### Authors' contributions

Prepared and edited the manuscript: Li T, Chan ASC, Meng SS

### Availability of data and materials

Not applicable.

### Financial support and sponsorship

This work was supported by the National Natural Science Foundation of China (22001269); the Research Foundation for Natural Science Foundation of Guangdong Province (2022A1515010597); (2023A1515030244).

### Conflicts of interest

All authors declared that there are no conflicts of interest.

### Ethical approval and consent to participate

Not applicable.

### Consent for publication

Not applicable.

### Copyright

© The Author(s) 2023.

## REFERENCES

1. Chirik P, Morris R. Getting down to earth: the renaissance of catalysis with abundant metals. *Acc Chem Res* 2015;48:2495. DOI PubMed
2. Ciftci M, Tasdelen MA, Yagci Y. Macromolecular design and application using  $Mn_2(CO)_{10}$ -based visible light photoinitiating systems. *Polym Int* 2016;65:1001-14. DOI
3. Carney JR, Dillon BR, Thomas SP. Recent advances of manganese catalysis for organic synthesis. *Eur J Org Chem* 2016;2016:3912-29. DOI
4. Li T, Zhang H, Chan AS, Meng S. Manganese-catalyzed dehydrogenative coupling of silanes and hydroxyl compound controlled by phosphine oxide. *Cell Rep Phys Sci* 2023;4:101313. DOI
5. Lu Q, Klauck FJR, Glorius F. Manganese-catalyzed allylation via sequential C-H and C-C/C-Het bond activation. *Chem Sci* 2017;8:3379-83. DOI PubMed PMC
6. Hu Y, Zhou B, Wang C. Inert C-H bond transformations enabled by organometallic manganese catalysis. *Acc Chem Res* 2018;51:816-27. DOI
7. Ge L, Harutyunyan SR. Manganese(i)-catalyzed access to 1,2-bisphosphine ligands. *Chem Sci* 2022;13:1307-12. DOI
8. Oates CL, Goodfellow AS, Bühl M, Clarke ML. Manganese catalysed enantioselective hydrogenation of *in situ*-synthesised imines: efficient asymmetric synthesis of amino-indane derivatives. *Green Chem* 2023;25:3864-8. DOI
9. Postolache R, Pérez JM, Castiñeira Reis M, Ge L, Sinnema EG, Harutyunyan SR. Manganese(I)-catalyzed asymmetric hydrophosphination of  $\alpha,\beta$ -unsaturated carbonyl derivatives. *Org Lett* 2023;25:1611-5. DOI PubMed PMC
10. Liu W, Ackermann L. Manganese-catalyzed C-H activation. *ACS Catal* 2016;6:3743-52. DOI
11. Crossley SW, Obradors C, Martínez RM, Shenvi RA. Mn-, Fe-, and Co-catalyzed radical hydrofunctionalizations of olefins. *Chem Rev* 2016;116:8912-9000. DOI PubMed PMC
12. Trovitch RJ. The Emergence of manganese-based carbonyl hydrosilylation catalysts. *Acc Chem Res* 2017;50:2842-52. DOI PubMed
13. Jamatia R, Mondal A, Srimani D. Visible-light-induced manganese-catalyzed reactions: present approach and future prospects. *Adv Synth Catal* 2021;363:2969-95. DOI
14. Bianchi R, Gervasio G, Marabello D. Experimental electron density analysis of  $Mn_2(CO)_{10}$ : metal-metal and metal-ligand bond characterization. *Inorg Chem* 2000;39:2360-6. DOI PubMed
15. Meckstroth WK, Ridge DP. Properties of ions and radicals derived from decacarbonyldimanganese, decacarbonylmanganeserhenium, and decacarbonyldirhenium by electron attachment and protonation in the gas phase. *J Am Chem Soc* 1985;107:2281-5. DOI
16. Hughey JL, Anderson CP, Meyer TJ. Photochemistry of  $Mn_2(CO)_{10}$ . *J Organomet Chem* 1977;125:C49-52. DOI
17. Fawcett JP, Poe A, Sharma KR. Reaction mechanisms of metal-metal bonded carbonyls. X. Thermal decomposition of decacarbonyldimanganese and decacarbonylmanganeserhenium in decalin. *J Am Chem Soc* 1976;98:1401-7. DOI
18. Asandei AD, Adebolu OI, Simpson CP. Mild-temperature  $Mn_2(CO)_{10}$ -photomediated controlled radical polymerization of vinylidene fluoride and synthesis of well-defined poly(vinylidene fluoride) block copolymers. *J Am Chem Soc* 2012;134:6080-3. DOI PubMed
19. McMahon CM, Renn MS, Alexanian EJ. Manganese-catalyzed carboacylations of alkenes with alkyl iodides. *Org Lett* 2016;18:4148-50. DOI PubMed PMC
20. Wang L, Lear JM, Rafferty SM, Fosu SC, Nagib DA. Ketyl radical reactivity via atom transfer catalysis. *Science* 2018;362:225-9. DOI PubMed PMC
21. Rafferty SM, Rutherford JE, Zhang L, Wang L, Nagib DA. Cross-selective aza-pinacol coupling via atom transfer catalysis. *J Am*

- Chem Soc* 2021;143:5622-8. DOI PubMed PMC
22. Nuhant P, Oderinde MS, Genovino J, et al. Visible-light-initiated manganese catalysis for C-H alkylation of heteroarenes: applications and mechanistic studies. *Angew Chem Int Ed Engl* 2017;56:15309-13. DOI PubMed
  23. Liu RZ, Li J, Sun J, et al. Generation and reactivity of amidyl radicals: manganese-mediated atom-transfer reaction. *Angew Chem Int Ed* 2020;59:4428-33. DOI PubMed
  24. Weng WZ, Liang H, Liu RZ, Ji YX, Zhang B. Visible-light-promoted manganese-catalyzed atom transfer radical cyclization of unactivated alkyl iodides. *Org Lett* 2019;21:5586-90. DOI PubMed
  25. Xie J, Han J, Han J, et al. Photoinduced manganese-catalysed hydrofluorocarbofunctionalization of alkenes. *Nat Synth* 2022;1:475-86. DOI
  26. Friestad GK, Marié JC, Suh Y, Qin J. Mn-mediated coupling of alkyl iodides and chiral N-acylhydrazones: optimization, scope, and evidence for a radical mechanism. *J Org Chem* 2006;71:7016-27. DOI PubMed
  27. Slater KA, Friestad GK. Mn-mediated radical-ionic annulations of chiral N-acylhydrazones. *J Org Chem* 2015;80:6432-40. DOI PubMed
  28. Ji YX, Li J, Li CM, Qu S, Zhang B. Manganese-catalyzed N-F bond activation for hydroamination and carboamination of alkenes. *Org Lett* 2021;23:207-12. DOI PubMed
  29. Mach K, Nováková J, Raynor J. Electron spin resonance spectroscopy of  $Mn(CO)_5 \cdot$  radicals generated in the gas phase thermolysis of  $Mn_2(CO)_{10}$ . *J Organomet Chem* 1992;439:341-5. DOI
  30. Fieldhouse SA, Fullam BW, Neilson GW, Symons MCR. Reaction of metal carbonyls with oxygen. *J Chem Soc, Dalton Trans* 1974:567-9. DOI
  31. Meng SS, Lin LR, Luo X, Lv HJ, Zhao JL, Chan ASC. Aerobic oxidation of alcohols with air catalyzed by decacarbonyldimanganese. *Green Chem* 2019;21:6187-93. DOI
  32. Song X, Meng S, Zhang H, Jiang Y, Chan ASC, Zou Y. Dibrominated addition and substitution of alkenes catalyzed by  $Mn_2(CO)_{10}$ . *Chem Commun* 2021;57:13385-8. DOI PubMed
  33. Yang X, Wang C. Dichotomy of manganese catalysis via organometallic or radical mechanism: stereodivergent hydrosilylation of alkynes. *Angew Chem Int Ed Engl* 2018;57:923-8. DOI PubMed
  34. Yang X, Wang C. Diverse fates of  $\beta$ -silyl radical under manganese catalysis: hydrosilylation and dehydrogenative silylation of alkenes. *Chin J Chem* 2018;36:1047-51. DOI
  35. Wu S, Zhang Y, Jiang H, et al. Manganese catalyzed dehydrogenative silylation of alkenes: Direct access to allylsilanes. *Tetrahedron Lett* 2020;61:152053. DOI
  36. Dong J, Yuan XA, Yan Z, et al. Manganese-catalysed divergent silylation of alkenes. *Nat Chem* 2021;13:182-90. DOI
  37. Liang H, Ji YX, Wang RH, Zhang ZH, Zhang B. Visible-light-initiated manganese-catalyzed E-selective hydrosilylation and hydrogermylation of alkynes. *Org Lett* 2019;21:2750-4. DOI PubMed
  38. Vivien A, Veyre L, Mirgalet R, Camp C, Thieuleux C.  $Mn_2(CO)_{10}$  and UV light: a promising combination for regioselective alkene hydrosilylation at low temperature. *Chem Commun* 2022;58:4091-4. DOI PubMed
  39. Zheng J, Chevance S, Darcel C, Sortais JB. Selective reduction of carboxylic acids to aldehydes through manganese catalysed hydrosilylation. *Chem Commun* 2013;49:10010-2. DOI PubMed
  40. Wei D, Buhaibeh R, Canac Y, Sortais JB. Manganese and rhenium-catalyzed selective reduction of esters to aldehydes with hydrosilanes. *Chem Commun* 2020;56:11617-20. DOI PubMed
  41. Ji YX, Wang LJ, Guo WS, Bi QR, Zhang B. Intermolecular iodofluoroalkylation of unactivated alkynes and alkenes mediated by manganese catalysts. *Adv Synth Catal* 2020;362:1131-7. DOI
  42. Dong J, Wang X, Wang Z, Song H, Liu Y, Wang Q. Visible-light-initiated manganese-catalyzed giese addition of unactivated alkyl iodides to electron-poor olefins. *Chem Commun* 2019;55:11707-10. DOI
  43. Wang X, Dong J, Li Y, Liu Y, Wang Q. Visible-light-mediated manganese-catalyzed allylation reactions of unactivated alkyl iodides. *J Org Chem* 2020;85:7459-67. DOI
  44. Wang X, Zhu B, Dong J, et al. Visible-light-mediated multicomponent reaction for secondary amine synthesis. *Chem Commun* 2021;57:5028-31. DOI
  45. Guo Y, Cao Y, Song H, Liu Y, Wang Q. Photoredox relay-catalyzed gem-difluoroallylation of alkyl iodides. *Chem Commun* 2021;57:9768-71. DOI PubMed
  46. Li CM, Dong XX, Wang Z, Zhang B. Visible light-initiated manganese-catalyzed hydrosulfonylation of alkenes. *Green Chem* 2023;25:4122-8. DOI